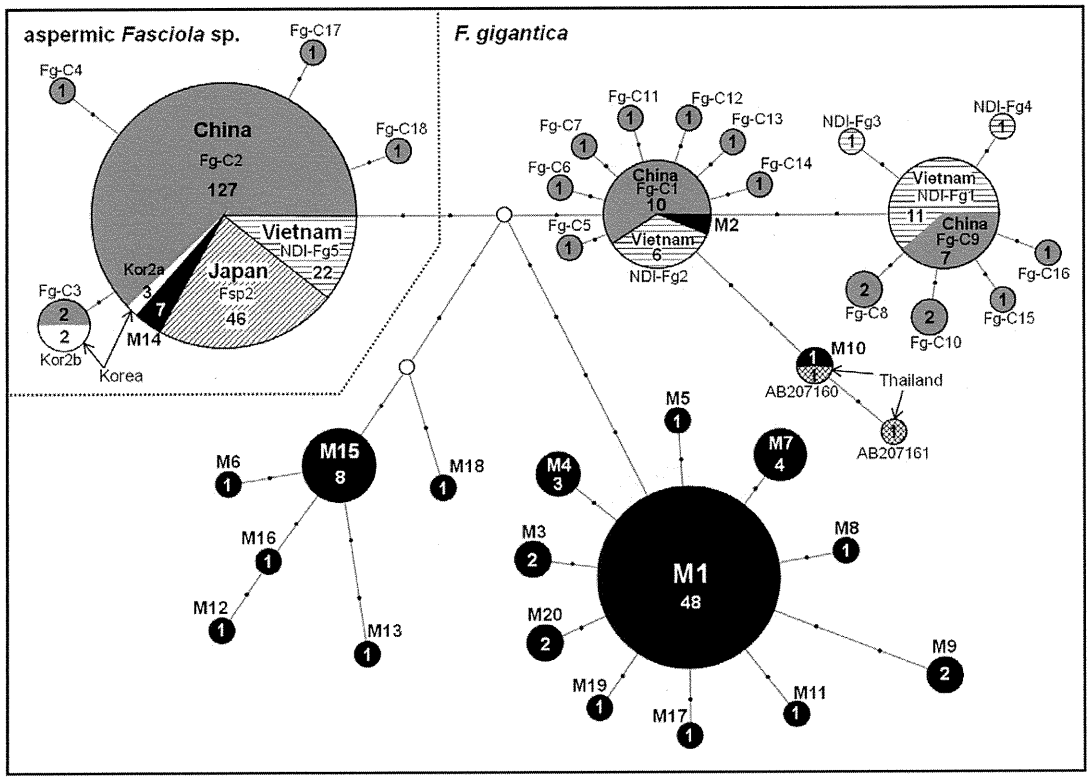

Fig. 4. A median-joining network constructed for the mitochondrial *nad1* haplotypes of *F. gigantica* and aspermic *Fasciola* sp. from Myanmar and other countries. Small black points on nodes indicate the number of nucleotide substitutions. White circles on nodes indicate median vectors. The Myanmar haplotypes obtained in this study are represented by black, and the haplotypes obtained from other Asian countries are shown in unique patterns: solid gray for China, solid white for Korea, horizontal for Vietnam, diagonal for Japan, and crosshatch for Thailand. The haplotype codes are shown adjacent to the circles. The haplotypes of aspermic *Fasciola* sp. are separated by dotted lines.

However, all of the Fst values showed significant *P* values ($p<0.01$), indicating that the 3 *F. gigantica* populations were significantly different.

4. Discussion

This study revealed that aspermic *Fasciola* sp. and *F. gigantica* were detected in Myanmar and that *F. gigantica* was predominant (90.9%, 80 out of 88 flukes). The 7 aspermic *Fasciola* sp. found in Myitkyina displayed Fg-M14 in the *nad1* haplotype, which is also present in aspermic *Fasciola* sp. from Japan (Fsp2), Korea (Kor2a), Vietnam (NDI-Fg5), and China (Fg-C2) [7,17–20]. These aspermic *Fasciola* sp. with identical *nad1* haplotypes are descendants of an ancestral maternal lineage. The lineage of aspermic *Fasciola* sp. is presumed to have spread through Asian countries with ancient artificial movement of definitive hosts, including domestic cattle [7,17–20], and to have appeared at least before the second century, the hypothesized period that the lineage was introduced into Japan via Korea with the ancestors of Japanese indigenous cattle [7]. However, it appeared that the lineage of aspermic *Fasciola* sp. detected in this study was an incidental finding and not established in Myitkyina, because the detection rates were very low in the infected hosts (5%, 1 out of 20 infected hosts) and in the flukes (8.0%, 7 out of 88 *Fasciola* flukes). The detection rates are generally high in countries where the lineage of aspermic *Fasciola* sp. is established: 40.0% of infected hosts in China [19], 53.6% of *Fasciola* flukes in Vietnam [20], and 76.7% of *Fasciola* flukes in Japan [7,18]. Therefore, we speculated that the host ruminant infected with the lineage of aspermic *Fasciola* sp. was presumably brought to Myitkyina from another country and sacrificed there. It can be inferred that the host came from China because Myitkyina is geographically adjacent to the southern part of China (see Fig. 2), and many Chinese residents reside there and participate in economic activities. This hypothesis is also supported by the fact that the 7 aspermic *Fasciola* sp. detected in Myitkyina displayed the Fh/Fg type, which was the major ITS1 type in Chinese aspermic *Fasciola* sp. [19]. Notably, this indicates that the lineage of aspermic *Fasciola* sp. may expand its distribution to non-endemic areas through migration of domestic animals.

In the MJ network, the 2 clades unique to Myanmar exhibited star-like expansions from the 2 founder haplotypes Fg-M1 and Fg-M15, suggesting that the 2 *F. gigantica* subpopulations in Myanmar recently experienced significant increases from the 2 founder haplotypes. It was speculated that the migration of the 2 founder haplotypes into Myanmar occurred independently because they were phylogenetically distinct. We hypothesized that limited numbers of *F. gigantica* possessing the 2 haplotypes were introduced into Myanmar through ancient anthropogenic movements of domestic ruminants and developed into the 2 unique *F. gigantica* subpopulations in Myanmar by demographic expansion. Although the migration route of *F. gigantica* into Myanmar remains unclear, zebu cattle (*Bos indicus*) appear to play a key role in expansion of *F. gigantica* into Asian countries [19]. In ancient period, international trades of Zebu cattle were probably very limited, which would contribute largely to construct unique *F. gigantica* populations in each country. Zebu cattle have been considered to be domesticated in India [27]. Hence, further phylogenetic studies on *Fasciola* flukes from other Asian countries,

Table 2
Pairwise fixation index (Fst values) between *F. gigantica* populations calculated from the nucleotide sequences of mitochondrial NADH dehydrogenase subunit 1 (*nad1*) gene.

	Myanmar	Vietnam
Vietnam	0.581 [a)]	
China	0.534 [a)]	0.105 [a)]

a) Siginificant *P* values ($P<0.01$).

including India, will reveal the evolution and expansion of *F. gigantica* in Asian countries. On the other hand, *F. gigantica* with Fg-M2 and Fg-M10 have apparently been introduced into Myanmar from neighboring countries through current artificial movements of domestic ruminants, because Fg-M2 and Fg-M10 were each detected in only 1 fluke and belong to clades of other Asian countries.

The 1 aspermic fluke from Yangon displayed Fg type in ITS1 and Fg-M3 in the *nad1* haplotype. Fg-M3 was also detected in *F. gigantica* collected in this study and belonged to one of the *F. gigantica* clades unique to Myanmar (Fig. 4). Therefore, we regarded this fluke as an abnormal *F. gigantica* having oligozoospermia, which might have been caused by aging of the fluke. This implies that in addition to spermatogenesis status and ITS1 type, analysis of the *nad1* haplotype is required to distinguish aspermic *Fasciola* sp. from *F. gigantica* with oligozoospermia caused by aging.

Acknowledgments

We are grateful to Dr. Khin Aung and the staff of LBVD in Myitkyina for their invaluable help in the collection of the *Fasciola* flukes. This study was supported in part by a Grant-in-Aid for Scientific Researches (B) (nos. 18405035, 22405037, and 2340544) from the Ministry of Education, Culture, Sports, Science, and Technology of Japan.

References

[1] Torgerson P, Claxton J. Epidemiology and Control. In: Dalton JP, editor. Fasciolosis. New York: CABI publishing; 1999. p. 113–49.
[2] Mas-Coma S, Valero MA, Bargues MD. *Fasciola*, lymnaeids and human fascioliasis, with a global overview on disease transmission, epidemiology, evolutionary genetics, molecular epidemiology and control. Adv Parasitol 2009;69:41–146.
[3] Terasaki K, Itagaki T, Shibahara T, Noda Y, Moriyama-Gonda N. Conparative study of the reproductive organs of *Fasciola* groups by optical microscope. J Vet Med Sci 2001;63:735–42.
[4] Adlard RD, Barker SC, Blair D, Cribb TH. Comparison of the second internal transcribed spacer (ribosomal DNA) from populations and species of Fasciolidae (Digenea). Int J Parasitol 1993;23:423–5.
[5] Itagaki T, Tsutsumi K. Triploid form of *Fasciola* in Japan: genetic relationships between *Fasciola hepatica* and *Fasciola gigantica* determined by ITS-2 sequence of nuclear rDNA. Int J Parasitol 1998;28:777–81.
[6] Marcilla A, Bargues MD, Mas-Coma S. A PCR-RFLP assay for the distinction between *Fasciola hepatica* and *Fasciola gigantica*. Mol Cell Probes 2002;16:327–33.
[7] Itagaki T, Kikawa M, Sakaguchi K, Shimo J, Terasaki K, Shibahara T, et al. Genetic characterization of parthenogenic *Fasciola* sp. in Japan on the basis of the sequences of ribosomal and mitochondrial DNA. Parasitology 2005;131:679–85.
[8] Watanabe S, Iwata S. *Fasciola* species in Japan. J Jpn Vet Med Assoc 1954;7:124–6 (in Japanese).
[9] Itagaki H, Akane S. Morphological study on the Japanese liver fluke, compared with African specimens. Bull Azabu Vet Coll 1959;6:115–23.
[10] Oshima T, Akahane H, Shimazu T. Patterns of the variation of the common liver fluke (*Fasciola* sp.) in Japan. I. Variations in the sizes and shapes of the worms and eggs. Jpn J Parasitol 1968;17:97–105 (in Japanese with English summary).
[11] Varma AK. On *Fasciola indica* n. sp. with some observation on *F. hepatica* and *F. gigantica*. J Helminthol 1953;27:185–98.
[12] Chu JK, Kim YK. Taxonomical study on the Fasciolidae in Korea. Korean J Parasitol 1967;5:139–46.
[13] Kimura S, Shimizu A, Kawano J. Morphological observation on liver fluke detected from naturally infected carabaos in the Philippines. Sci Rept Fac Agr Kobe Univ 1984;16:353–7.
[14] Ashrafi K, Valero MA, Panova M, Periago MV, Massoud J, Mas-Coma S. Phenotypic analysis of adults of *F. hepatica*, *F. gigantica* and intermediate forms from the endemic region of Gilan, Iran. Parasitol Int 2006;55:249–60.
[15] Terasaki K, Moriyama-Gonda N, Noda Y. Abnormal spermatogenesis in the common liver fluke (*Fasciola* sp.) from Japan and Korea. J Vet Med Sci 1998;60: 1305–9.
[16] Terasaki K, Akahane H, Habe S. The geographical distribution of common liver flukes (the Genus *Fasciola*) with normal abnormal spermatogenesis. Jpn J Vet Sci 1982;44:223–31.
[17] Itagaki T, Kikawa M, Terasaki K, Shibahara T, Fukuda K. Molecular characterization of parthenogenetic *Fasciola* sp. in Korea on the Basis of DNA sequences of ribosomal ITS1 and Mitochondrial ND I Gene. J Vet Med Sci 2005;67:1115–8.
[18] Ichikawa M, Iwata N, Itagaki T. DNA types of aspermic *Fasciola* species in Japan. J Vet Med Sci 2010;72:1371–4.
[19] Peng M, Ichinomiya M, Ohtori M, Ichikawa M, Shibahara T, Itagaki T. Molecular characterization of *Fasciola hepatica*, *Fasciola gigantica*, and aspermic *Fasciola* sp. in China based on nuclear and mitochondrial DNA. Parasitol Res 2009;105:809–15.
[20] Itagaki T, Salaguchi K, Terasaki K, Sasaki O, Yoshihara S, Van Dung T. Occurrence of spermic diploid and aspermic triploid forms of *Fasciola* in Vietnam and their molecular characterization based on nuclear and mitochondrial DNA. Parasitol Int 2009;58:81–5.
[21] Ichikawa M, Itagaki T. Discrimination of the ITS1 types of *Fasciola* spp. based on a PCR-RFLP method. Parasitol Res 2010;106:757–61.
[22] Larkin MA, Blackshields G, Brown NP, Chenna R, McGettigan PA, McWilliam H, et al. Clustal W and Clustal X version 2.0. Bioinformatics 2007;23:2947–8.
[23] Telford MJ, Herniou EA, Russel RB, Littlewood DT. Changes in mitochondrial genetic codes as phylogenetic characters: two examples of from the flatworms. Proc Natl Acad Sci U S A 2000;97:11359–113364.
[24] PAUP* Swofford DL. Phylogenetic analysis using parasimony and other methods ver. 4.0beta. Sunderland, Massachussetts: Sinauer Associates; 2001.
[25] Bandelt HJ, Forster P, Rohl A. Median-joining networks for inferring intraspecific phylogenies. Mol Biol Evol 1999;16:37–48.
[26] Excoffier L, Lischer HEL. Arlequin suite ver 3.5: A new series of programs to perform population genetics analyses under Linux and Windows. Mol Ecol Res 2010;10:564–7.
[27] Chen S, Lin BZ, Baig M, Mitra B, Lopes RJ, Santos AM, et al. Zebu cattle are an exclusive legacy of the South Asia Neolithic. Mol Biol Evol 2010;27:1–6.

[Research Note]

Morphological and molecular characterization of sylvatic isolates of *Trichinella* T9 obtained from feral raccoons (*Procyon lotor*)

Tomoko Kobayashi[1,2], Yuta Kanai[3,4], Yuzaburo Oku[3,5], Yohei Matoba[1], Ken Katakura[3] and Mitsuhiko Asakawa[1*]

The genus *Trichinella* (Trichinellidae: Trichinellidea: Enoplida) has a worldwide distribution in domestic and/or sylvatic animals, and it was once believed to be a monospecific group, but this genus now comprises eight species (*Trichinella spiralis, T. nativa, T. britovi, T. murrelli, T. nelsoni, T. pseudospiralis, T. papuae, T. zimbabwensis*) and three additional genotypic variants (T6, T8, T9) that have yet to be taxonomically defined (Pozio and Zarlenga, 2005). Among them, there are two taxa of *Trichinella* in Japan, namely *Trichinella* T9 from raccoon dogs (*Nyctereutes procyonoides viverrinus* and *N. p. albus*), black bears (*Ursus thibetanus*), brown bears (*U. arctos yesoensis*) and foxes (*Vulpes vulpes schrencki*), and *T. nativa* from a red fox (*V. vulpes*) (Nagano *et al.*, 1999; Kanai *et al.*, 2006). Previous work has shown that raccoons (*Procyon lotor*), which have been introduced from North America since the 1970s, are involved in the sylvatic cycle of *Trichinella* in Japan (Kobayashi *et al.*, 2007). We present here additional morphological and molecular analyses of these sylvatic isolates of *Trichinella* from feral raccoons in Hokkaido, Japan.

In the present study, five *Trichinella* isolates that originated from 648 feral raccoons captured in 2004 and 2005 in Hokkaido, Japan were analyzed. *Trichinella* larvae were examined by an artificial digestion method using tongue muscle (Henriksen, 1978). Briefly, individual tongue samples were digested in 1% pepsin-HCl solution with constant gentle stirring for at least 4 hr at 37°C. After the muscle tissues had been digested, the sediment was allowed to settle and was washed several times. The sediment from the last washing was examined for larvae under a dissection microscope. The larvae were preserved in ethanol for morphological examination and as voucher specimens (Reg. Nos. AS 4324, 5342, 5417, 5498, and 5601) in the Wild Animal Medical Center, Rakuno Gakuen University, Japan. Measurements of cyst size were made from the muscular tissue placed on a glass slide under a dissection microscope. Some of the larvae collected were preserved in TE buffer at –30°C until use, and DNA was extracted from five single larvae according to a previously described method (Bandi *et al.*, 1995; Kanai *et al.*, 2006). These larvae were analyzed separately by a multiplex polymerase chain reaction (PCR) following the method of Zarlenga *et al.* (1999). The five sets of primers listed in Table 1 were used for the multiplex PCR with 10 pmol/μl of each primer. Amplification was carried out using *Taq* polymerase (QIAGEN) with Minicycler™ (MJ Research) under the following conditions: preheating at 94°C for 30 sec, annealing at 58°C for 30 sec, and elongation at 72°C for 1 min for 35 cycles. The PCR amplicon was separated by 2.5% agarose gel electrophoresis and stained with ethidium bromide. For further characterization, the nucleotide sequence of a partial mitochondrial cytochrome oxidase subunit I (COI) was determined. Primers (5'-CAC CCA GAA GTA TAC ATC C-3' and 5'-GTA ATA ATA GGT CTA GGG AGG-3') designed based on sequences of *T. nativa* (accession no. DQ007891) and *Trichinella* T9 (DQ 007898) were used for amplification and nucleotide sequencing. PCR was performed under the following conditions: preheating at 94°C for 5 min, denaturation at 94°C for 1 min, annealing at 50°C for 1 min, and elongation at 72°C for 1 min for 40 cycles. PCR products were purified and directly sequenced using DTCS Quick Start Master Mix (BECKMAN COULTER™) with an automatic sequencer (CEQ™ 8000, BECKMAN COULTER™) according to the manufacturers' instructions. All sequences were aligned using GENETYX-Mac ver. 10.1.4 software.

Table 1. Primer pairs used for multiplex PCR (Zarlenga *et al.*, 1999).

Primer pairs	Sequences
I	5'-GTTCCATGTGAACAGCAGT-3
	5'-CGAAAACATACGACAACTGC-3
II	5'-GCTACATCCTTTTGATCTGTT-3
	5'-AGACACAATATCAACCACAGTACA-3
III	5'-GCGGAAGGATCATTATCGTGTA-3
	5'-TGGATTACAAAGAAAACCATCACT-3
IV	5'-GTGAGCGTAATAAAGGTGCAG-3
	5'-TTCATCACACATCTTCCACTA-3
V	5'-CAATTGAAAACCGCTTAGCGTGTTT-3
	5'-TGATCTGAGGTCGACATTTCC-3

Larval cysts which formed in tongue muscles were spindle-shaped and each cyst included a single coiled larva.

[1] Department of Pathobiology, School of Veterinary Medicine, Rakuno Gakuen University, Hokkaido 060-8501, Japan.
[2] Present address: Research Team for Zoonotic Diseases, National Institute of Animal Health, National Agriculture and Food Research Organization (NARO), Kannondai, Tsukuba, Ibaraki 305-0856, Japan.
[3] Graduate School of Veterinary Medicine Laboratory of Parasitology Hokkaido University, Hokkaido 060-0818, Japan.
[4] Present address: Section of Viral Infections, Thailand-Japan Research Collaboration Center on Emerging and Re-emerging Infections (RCCERI), Nonthaburi, Thailand.
[5] Present address: Faculty of Agriculture Tottori University, Tottori 680-8553, Japan.
* Corresponding author, e-mail: askam@rakuno.ac.jp

Table 2. The measurements of *Trichinella* larvae obtained from the masseter of the raccoon AS4324 (in mm, n = 10).

	Max	Min	Mean	SD
Cyst length	0.47	0.3	0.336	0.046
Cyst width	0.26	0.2	0.233	0.018
Body length	1.25	0.65	1.056	0.185
Body width	0.04	0.03	0.036	0.003
Esophagus	1.12	0.46	0.774	0.036
Stichosome	0.9	0.36	0.61	0.01
Rectum	0.06	0.03	0.041	0.156

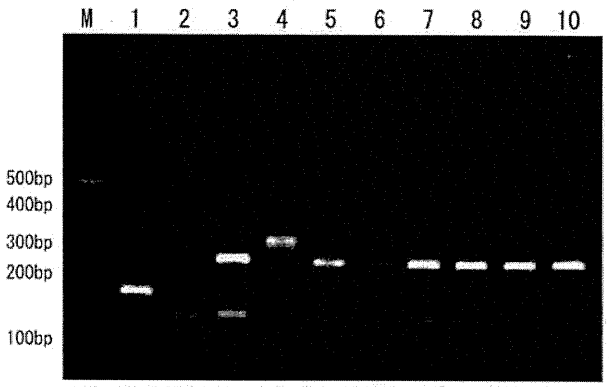

Fig. 1. Electrophoretic pattern after multiplex-PCR amplification of *Trichinella* larvae from feral raccoons and wildlife of Hokkaido Prefecture.
Lane M: 100 bp DNA ladder, lane 1: *T. spiralis* reference larva (code ISS 413), lane 2: *T. nativa* (control, Otofuke fox: Kanai *et al.*, unpublished), lane 3: T9 (control, Sapporo fox: Kanai *et al.* 2007), lane 4: *T. pseudospiralis* (code ISS 13), lane 5: AS5342, lane 6: AS5417, lane 7: AS5498, lane 8: AS4324, lane 9: AS5601, lane 10: T9 (control, Atsuma raccoon dog: Kobayashi *et al.*, unpublished)

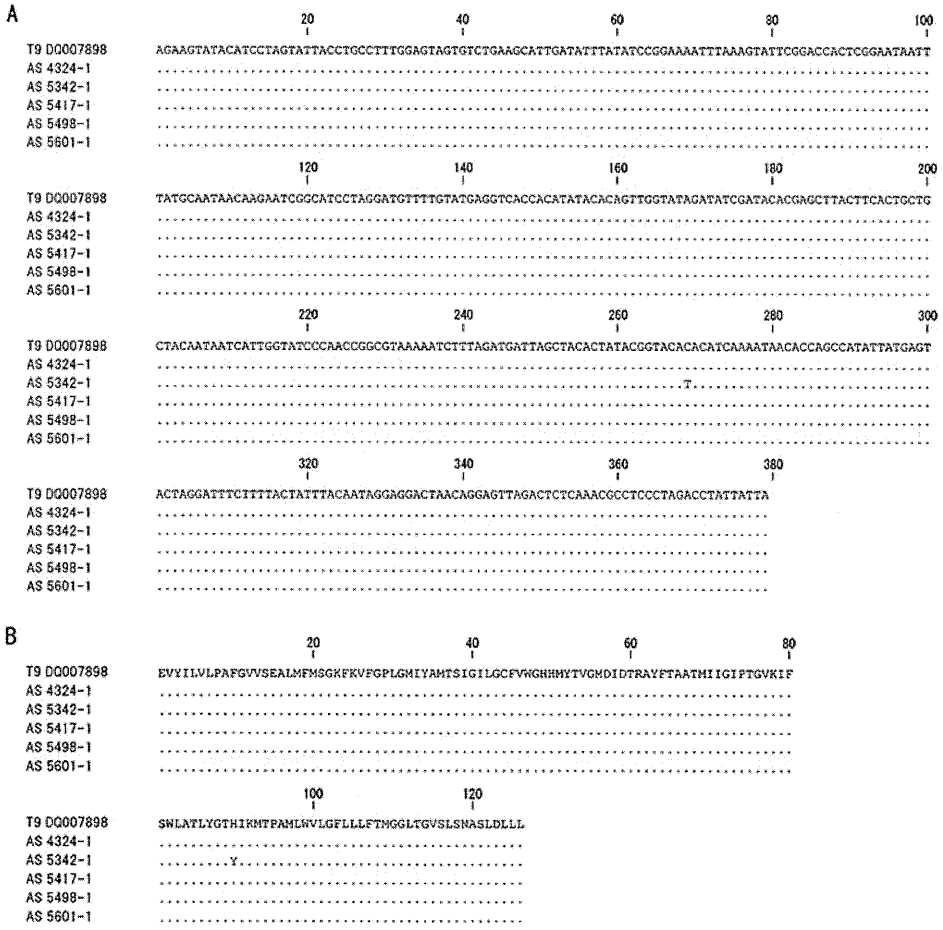

Fig. 1. Alignment of a partial COI sequence of the *Trichinella* larvae.
Nucleotide (A) and amino acid (B) alignments of a partial COI sequence of the *Trichinella* larvae of feral raccoons from Hokkaido with *Trichinella* T9 (accession number DQ007898). Bases that are identical to those of T9 are indicated by dots.

The measurements of the larvae and the cysts are shown in Table 2. Muscle larvae from infected raccoons showed two bands of 127 bp and 253 bp; a pattern specific to *T. britovi* complex (*T. britovi*, T8, T9) (Fig. 1). The nucleotide sequences of a part of the COI gene (379 bp) of larvae from the five raccoons showed highest identities (99.7-100%) to *Trichinella* T9; indeed, the COI sequences of *Trichinella* T9 from five raccoons showed little divergence (Fig. 2). Of the five samples, four (WAMC-AS nos. 4324-1, 5417-1, 5498-1, and 5601-1) had the same sequence (accession number AB 267878), which was completely identical to the previously reported sequences of *Trichinella* T9 from animals of mainland Japan (Nagano *et al.*, 1999). A DNA sequence of *Trichinella* T9 from the remaining sample (WAMC-AS no. 5342-1) showed a single nucleotide polymorphism, which resulted in a single amino acid polymorphism (accession number AB 267879). DNA sequencing of the three other larvae from the same raccoons were analyzed by the same method, and showed the same pattern. *Trichinella* larvae from feral raccoons of Japan were identified by multiplex PCR and COI sequence as *Trichinella* T9.

Raccoons are widely distributed throughout North America, and have also been introduced to Russia and Western Europe. Previously, *T. murrelli* (Pozio and La Rosa, 2000) and *T. psudospiralis* (Garkavi and Gineev, 1976) have been reported in feral raccoons of North America and Russia, respectively. *Trichinella murrelli* is the etiological agent of infection in sylvatic carnivores living in temperate areas of the Nearctic region and *T. psudospiralis* is a cosmopolitan non-encapsulated species infecting both mammals and birds. However, neither *T. murrelli* nor *T. psudospiralis* but T9 has been determined in feral raccoons in Japan. Since *Trichinella* T9 has been reported only in wildlife indigenous to Japan (*i.e.*, a raccoon dog from Yamagata, a black bear from Aomori, and raccoon dogs and foxes from Hokkaido) (Nagano *et al.*, 1999; Kanai *et al.*, 2006), the present results suggested that the raccoons tested here acquired the larvae in the natural ecosystem of Japan.

ACKNOWLEGDEMENTS

The present survey was supported in part by Grant-in-Aid (nos. 14560271, 18510205, S0891002) and by the High Technological Research Center (Rakuno Gakuen Univ.) of The Ministry of the Education, Science and Culture of Japan. We are grateful for the raccoon samples provided to us by the local government offices, EnVision, Hokkaido Forest Management Corporation, Nopporo Natural Forest Park Office, and Raccoon Research Group. We are also grateful to Y. Asakawa, K. Suzuki, G. Abe, and M. Sashika for sampling.

LITERATURE CITED

Bandi, C., La Rosa, G., Bardin, M.G., Damiani, G., Cominicini, S., Tasciotti, L. and Pozio, E. (1995) Random amplified polymorphic DNA fingerprints of the eight taxa of *Trichinella* and their comparison with allozyme analysis. Parasitology 110, 401-407.

Garkavi, A. M. and Gineev, B. L. (1976) *Trichinella* in wild animals in northern Caucasus. Voprosy Prirodnoi Ochagovosti Boleznei 8, 136-139.

Henriksen, S. A. (1978) Recovery of *Trichinella spiralis* larvae from frozen muscle samples. Acta Veterinaria Scandinavica 19, 466-468.

Kanai, Y., Nonaka, N., Katakura, K. and Oku, Y. (2006) *Trichinella nativa* and *Trichinella* T9 in the Hokkaido island, Japan. Parasitology International 55, 313-315.

Kobayashi, T., Kanai, Y., Ono, Y., Matoba, Y., Suzuki, K., Okamoto, M., Taniyama, H., Yagi, K., Oku, Y., Katakura, K. and Asakawa, M. (2007) Epidemiology, histopathology, and muscle distribution of *Trichinella* T9 in feral raccoons (*Procyon lotor*) and wildlife of Japan. Parasitology Research 100, 1287-1291.

Nagano, I., Wu, Z., Matsuo, A., Pozio, E. and Takahashi, Y. (1999) Identification of *Trichinella* isolates by polymerase chain reaction--restriction fragment length polymorphism of the mitochondrial cytochrome c-oxidase subunit I gene. International Journal for Parasitology 29, 1113-1120.

Pozio, E. and Zarlenga, D. S. (2005) Recent advances on the taxonomy, systematics and epidemiology of *Trichinella*. International Journal for Parasitology 35, 1191-1204.

Pozio, E. and La Rosa, G. (2000) *Trichinella murrelli* n. sp: etiological agent of sylvatic trichinellosis in temperate areas of North America. The Journal of Parasitology 86, 134-139.

Zarlenga, D. S., Chute, M. B., Martin, A. and Kapel, C. M. O. (1999) A multiplex PCR for unequivocal differentiation of all encapsulated and non-encapsulated genotypes of *Trichinella*. International Journal for Parasitology 29, 1859-1867.

Received January 15, 2011

J Nat Med (2012) 66:233–240
DOI 10.1007/s11418-011-0571-5

NOTE

Antitrypanosomal activities of acetylated bruceines A and C; a structure–activity relationship study

Ahmed Elkhateeb · Yusuke Tosa · Hideyuki Matsuura · Kensuke Nabeta · Ken Katakura

Received: 10 May 2011 / Accepted: 15 July 2011 / Published online: 6 August 2011

Abstract The crude extract of *Brucea javanica* showed strong in vitro inhibitory activity against *Trypanosoma evansi*. Among the isolated quassinoids, bruceines A, C, and bruceantinol were found to be the most potent compounds against *T. evansi*. To gain a deeper understanding of the relationship between the free hydroxyl groups and the activity, several *O*-acetylated derivatives of bruceines A and C were synthesized and their in vitro antitrypanosomal activities against trypomastigotes of *T. evansi* were examined and compared with those of the original compounds. The following structure–activity relationships were observed: (1) the free hydroxyl groups at positions C-3, C-11, and C-12 are essential for antitrypanosomal activity; (2) the C-11 and C-12 hydroxyl groups are more important for the activity than the enolic hydroxyl group at C-3, and; (3) the free hydroxyl group at C-4′ of bruceine C does not have any significant effect on the activity.

Keywords *Brucea javanica* · Simaroubaceae · Quassinoids · Antitrypanosomal activity · *Trypanosoma evansi*

A. Elkhateeb · Y. Tosa · K. Katakura
Laboratory of Parasitology, Department of Disease Control, Graduate School of Veterinary Medicine, Hokkaido University, Sapporo 060-0818, Japan

A. Elkhateeb
Phytochemistry and Plant Systematic Department, National Research Centre, Dokki, Giza, Egypt

H. Matsuura (✉) · K. Nabeta
Laboratory of Bioorganic Chemistry, Division of Applied Bioscience, Graduate School of Agriculture, Hokkaido University, Sapporo 060-8589, Japan
e-mail: matsuura@chem.agr.hokudai.ac.jp

Introduction

Trypanosoma evansi is a flagellated, animal-pathogenic protozoan parasite. It infects a variety of large animals, including equines, camels, cattle, buffaloes, goats, sheep, and pigs, causing the form of trypanosomiasis known as surra, and is transmitted by blood-sucking insects of the genera *Tabanus*, *Stomoxys*, *Atylotus*, and *Lyperosia*. The disease leads to great financial losses in areas of Africa, Asia, and South America, where thousands of animals die from *T. evansi* infections [1]. It rarely causes disease in humans; the first case of human infection by *T. evansi* was reported in India in 2004 [2]. Currently, the drugs most commonly used for the treatment of *T. evansi* infection are diminazene aceturate, suramin, and quinapyramine. However, these drugs usually cause pronounced and severe side effects, and drug-resistant trypanosomes have developed in many regions [3]. Therefore, an alternative affordable chemotherapeutic agent with fewer side effects is urgently needed for the treatment of *T. evansi* infection. One possible source of such a treatment is plant extracts.

Brucea javanica (L.) Merr. (Simaroubaceae) is widely distributed throughout Asia. The bitter fruits of *B. javanica* (known as "ya dan zi") are used in traditional medicine for various ailments, including cancer, amoebic dysentery, and malaria [4, 5]. In common with other Simaroubaceae species, the bitter principles of this plant are due to quassinoids.

Recently, our research group examined the fruits of *B. javanica* for their antitrypanosomal properties. The crude extract of *B. javanica* showed strong in vitro inhibitory activity against *T. evansi*. Among the isolated quassinoids, bruceines A (**1**), C (**2**), and bruceantinol (**3**) were found to be the most potent compounds against *T. evansi* [6].

In our previous studies, the following structure–activity relationships for quassinoids in relation to the growth

inhibition of the parasite *T. evansi* were concluded: activity is influenced by the nature of the C-15 side chain and the nature of the A ring modification [6]. However, there was no information about the effects of the hydroxyl groups at positions C-3, C-11, C-12, and C-4′ on antitrypanosomal activity. Therefore, in the current study, a series of acetylated derivatives of bruceines A and C were synthesized, and their in vitro antitrypanosomal activities were compared with those of the original bruceines.

Results and discussion

Acetylation of compounds **1–3** was carried out using acetic anhydride in pyridine and CH_2Cl_2 in the presence of a catalytic amount of 4-dimethylaminopyridine (DMAP). The peracetate derivatives were obtained by using excess amounts of acetic anhydride; however, the mono and diacetyl derivatives were obtained by using one or two equivalents of acetic anhydride.

The molecular formula of 3,11,12,4′-tetra-*O*-acetyl bruceine C (**4**) was determined as $C_{36}H_{44}O_{16}$ from FAB-HRMS data. The difference between the FAB-MS *m/z* values of **2** and **4** suggests that four acetyl groups exist in the structure of **4**. The positions of the acetyl groups in **4** were determined as C-3, C-11, C-12, and C-4′, due to the downfield shifts of the H-11 (δ 5.20), H-12 (δ 5.30), and C-4 (δ 142.3) signals and the upfield shifts of H-2′ (δ 5.73) and C-2 (δ 187.8) when compared with the spectrum of **2**. In the same manner, the positions of the acetyl groups were unambiguously determined by comparing the NMR and mass spectral data of the acetylated derivatives with those of the starting compounds. The ^{13}C NMR spectrum of compound **5** showed a downfield shift of C-4 (δ 142.2) and an upfield shift of C-2 (δ 189.3) with respect to that of bruceine C (**2**), confirming the acetylation at *O*-C3.

The enolic hydroxyl group at C-3 of bruceine C (**2**) was selectively protected as a *tert*-butyldimethylsilyl (TBDMS) ether, **7** [7]. The molecular formula of **7** was determined as $C_{34}H_{51}O_{12}Si$ from its FAB-HRMS data. The difference between the FAB-MS *m/z* values of **2** and **7** suggests that one TBDMS group exists in the structure of **7**. The downfield shift of C-4 (δ 136.2) confirmed that the hydroxyl group at C-3 was selectively protected. Acetylation of compound **7** leads to the formation of its diacetyl derivative (**8**). In its ^1H NMR spectrum, compound **8** showed downfield shifts in H-11 (δ 5.20) and H-12 (δ 5.27); however, H-2′ (δ 6.02) remains intact with respect to that of **7**; in the case of 4′-*O*-Ac derivatives, H-2′ appears to be shifted upfield, as in compound **4**. This confirms that **8** is an 11,12-di-*O*-acetyl derivative of compound **7**. Removal of the protecting group was achieved by treating **8** with tetrabutylammonium fluoride in tetrahydrofuran to afford **9**. In the same manner, protecting the C-3 hydroxyl group of bruceine A (**1**), followed by acetylation in the presence of one equivalent of acetic anhydride and deprotection lead to the formation of 12-*O*-acetyl bruceine A (**16**). In its ^1H-NMR spectrum, compound **16** showed a downfield shift in H-12 (δ 5.28) compared with that of **1**, confirming the acetylation position is at *O*-C-12.

The antitrypanosomal activities of compounds **1–3** and their acetyl derivatives against *T. evansi* are shown in Fig. 1. Comparing the IC_{50} value of bruceine C (**2**) with that of its peracetate derivative (**4**) confirmed that the free hydroxyl groups are essential for antitrypanosomal activity. However, it was very important to check the effect of the acetylation of each of the hydroxyl groups at positions C-3, C-11, C-12, and C-4′ on the activity. Therefore; taking bruceine C (**2**) as an example, and noting the differences in the reactivities of the four hydroxyl groups [8], its mono and diacetyl derivatives at different positions were synthesized, and their activities were compared with each other and with that of bruceine C.

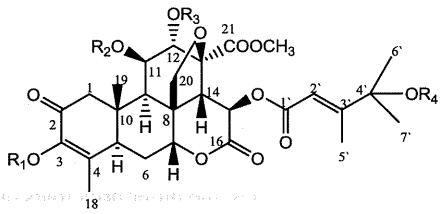

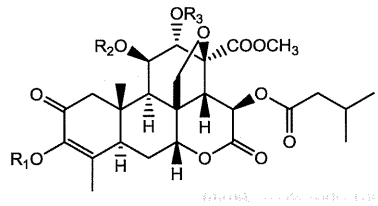

Fig. 1 Chemical structures and in vitro antitrypanosomal activities of bruceines A, C and their acetylated derivatives against *T. evansi*

Compound	IC_{50} (μg/mL)
2: R_1=R_2=R_3=R_4=H	0.019
3: R_1=R_2=R_3=H; R_4=Ac	0.035
5: R_1=Ac; R_2=R_3= R_4=H	0.26
10: R_1=R_4=Ac; R_2=R_3=H	0.29
6: R_1=R_3=Ac; R_2=R_4=H	8.71
9: R_1=R_4=H; R_2=R_3=Ac	17.29
4: R_1=R_2=R_3=R_4=Ac	34.78

Compound	IC_{50} (μg/mL)
1: R_1=R_2=R_3=H	0.017
12: R_1=Ac; R_2=R_3=H	0.56
16: R_1=R_2=H; R_3=Ac	5.49
13: R_1=R_3=Ac; R_2=H	20.29
11: R_1=R_2=R_3=Ac	68.41

3-*O*-acetyl bruceine C (**5**) showed greater activity than 3,12-di-*O*-acetyl bruceine C (**6**) and 3, 11,12,4′-tetra-*O*-acetyl bruceine C (**4**), respectively, indicating that as the number of free hydroxyl groups increases the activity increases. Comparing the activities of bruceine C (**2**), bruceantinol (4′-*O*-acetyl bruceine C, **3**), 3-*O*-acetyl-bruceine C (**5**), and 3-*O*-acetyl bruceantinol (**10**) confirmed that the effect of the free hydroxyl group at C-4′ of the ester side chain at C-15 on the activity is insignificant. Interestingly, it was found that 3,12-di-*O*-acetyl bruceine C (**6**) is twice as active as 11,12-di-*O*-acetyl-bruceine C (**9**), which indicates that the free hydroxyl group at C-11 is more important for the activity than the enolic hydroxyl group at C-3.

In the same manner, the mono-, di-, and triacetyl derivatives of bruceine A were found to be less active than bruceine A (**1**), confirming the importance of the free hydroxyl groups.

3-*O*-acetyl bruceine A (**12**) was found to be ten times more active than 12-*O*-acetyl bruceine A (**16**), which indicated that the free hydroxyl group at C-12 is more important for the activity than the enolic hydroxyl group at C-3.

Conclusion

In the present study, we prepared several acetylated derivatives of bruceines A and C, and evaluated their antitrypanosomal activities. Thus, the following structure–activity relationships were concluded: (1) the free hydroxyl groups at positions C-3, C-11, and C-12 are essential for antitrypanosomal activity; (2) the C-11 and C-12 hydroxyl groups are more important for the activity than the enolic hydroxyl group at C-3, and; (3) the free hydroxyl group at C-4′ of bruceine C does not have any significant effect on the activity.

We are currently studying the mechanism of action of these bruceines. However, it has been necessary to chemically modify their structures without affecting their activities significantly. One possible target for modification was provided by the free hydroxyl groups. Due to its higher reactivity (resulting from the enolic hydroxyl moiety), and its relatively minor effect on the activity compared to the C-11 and C-12 hydroxyl groups, the C-3 hydroxyl group is the most suitable of the free hydroxyl groups to modify.

Experimental

General

Mass spectra were measured on JEOL JMS-SX102A and JMS-AX500 spectrometers. NMR spectra were recorded in $CDCl_3$ on a JEOL JNM-EX 270 FT-NMR and on a Bruker AM-500 FT-NMR spectrometer. ^1H and ^{13}C chemical shifts were referenced to the solvent ($CDCl_3$, 7.24 and 77.0 ppm; respectively). Column chromatography was conducted with silica gel 60 (Kanto Chemical). Analytical thin-layer chromatography was performed on silica gel 60 F_{254} (Merck).

Plant material

Fruits of *Brucea javanica* were purchased from a local shop in Myanmar in April 2009.

Extraction and isolation

Dried ground fruits of *B. javanica* (2 kg) were defatted with *n*-hexane (3 L × 3), the marc was extracted with boiling water (8 L) for 30 min, and the same material was re-extracted in the same manner. The extract was filtered and concentrated up to 1 L under reduced pressure, and then partitioned with EtOAc (1 L × 4). The EtOAc layer was dried over anhydrous Na_2SO_4 and then concentrated under reduced pressure. The obtained residue (12.15 g) was chromatographed on a silica gel column and eluted with $CHCl_3$, MeOH-$CHCl_3$ (3:97), MeOH-$CHCl_3$ (20:80), and MeOH successively. The MeOH-$CHCl_3$ (3:97) extract (2.16 g) was rechromatographed on silica gel using EtOAc–hexane (80:20) to give three fractions (Fr. I–III). Fr. I was recrystallized from MeOH to give pure compound **1** (400 mg). Fractions II and III were found to contain pure compounds **3** (150 mg) and **2** (350 mg), respectively.

In vitro test for antitrypanosomal activity

The in vitro assay against *Trypanosoma evansi* was described in detail in a previous paper [6].

Synthesis of the acetyl derivatives of compounds **1–3**

3,11,12,4′-Tetra-O-acetyl bruceine C (4)

Acetic anhydride (0.5 mL, 5.0 mmol) was added to a solution of bruceine C (**2**) (45 mg, 0.08 mmol), a catalytic amount of DMAP (15 mg, 0.12 mmol), and pyridine (0.5 mL) in CH_2Cl_2 (2.0 mL). After being stirred at room temperature for 20 h, the reaction mixture was dissolved in EtOAc (30 mL) and washed with 1 M HCl (20 mL × 3), $NaHCO_3$ (20 mL × 2), and brine. The aqueous extracts were collected and re-extracted with EtOAc (50 mL × 4). The organic extracts were collected, dried over anhydrous Na_2SO_4, and chromatographed (SiO_2, 80% EtOAc/hexane) to afford 28 mg of compound **4** (48%, white amorphous powder).

^{1}H NMR (270 MHz, $CDCl_3$) δ 6.05 (1H, br s, H-15), 5.73 (1H, s, H-2′), 5.30 (1H, s, H-12), 5.20 (1H, d, J = 4.9 Hz, H-11), 4.83(1H, s, H-7), 4.75 (1H, d, J = 7.7 Hz, H_a-20), 3.84 (1H, d, J = 7.7 Hz, H_b-20), 3.71 (3H, s, OCH_3), 3.26 (1H, br d, J = 12.4 Hz, H-14), 3.07 (1H, br d, J = 12.2 Hz, H-5), 2.64 (1H, d, J = 15.5 Hz, H_β-1), 2.42 (1H, m, H_α-6), 2.37 (1H, d, J = 15.5 Hz, H_α-1), 2.25 (3H, s, $COCH_3$), 2.12 (3H, s, H-5′), 2.09 (3H, s, $COCH_3$), 2.07 (1H, br s, H-9), 1.99 (3H, s, $COCH_3$) 1.98 (3H, s, $COCH_3$), 1.84 (1H, m, H_β-6), 1.78 (3H, s, H-18), 1.51 (3H, s, H-6′), 1.46 (3H, s, H-7′), 1.29 (3H, s, H-19); ^{13}C NMR (67.5 MHz, $CDCl_3$) δ 187.8 (C-2), 169.4 (C-21), 168.9 ($OCOCH_3$), 168.7 ($OCOCH_3$), 168.5 ($OCOCH_3$), 167.8 ($OCOCH_3$), 166.7 (C-16), 165.8 (C-1′), 164.5 (C-3′), 144.7 (C-3), 142.3(C-4), 111.6 (C-2′), 82.4 (C-4′), 82.0 (C-7), 79.8 (C-13), 73.5 (C-20), 70.7 (C-12), 69.0 (C-11), 65.7 (C-15), 53.1 (OCH_3), 51.2 (C-14), 50.1 (C-1), 45.0 (C-8), 42.9 (C-5), 41.3 (C-9), 40.2 (C-10), 28.6 (C-6), 26.4 (C-6′), 25.8 (C-7′), 21.6 ($OCOCH_3$), 21.4 ($OCOCH_3$), 20.5 ($OCOCH_3$), 20.2 ($OCOCH_3$), 15.6 (C-19), 14.5 (C-18), 14.4 (C-5′); HRFABMS m/z 755.2514 $[M + Na]^+$ (calcd for $C_{36}H_{44}O_{16}Na$, 755.2527).

*3-O-Acetyl bruceine C (**5**) and 3,12-di-O-acetyl bruceine C (**6**)*

Acetic anhydride (20 μL, 0.2 mmol) was added to a solution of bruceine C (**2**) (45 mg, 0.08 mmol), a catalytic amount of DMAP (15 mg, 0.12 mmol), and pyridine (0.2 mL) in CH_2Cl_2 (2.0 mL). After being stirred at room temperature for 20 h, the reaction mixture was dissolved in EtOAc (30 mL) and washed with 1 M HCl (20 mL × 3), $NaHCO_3$ (20 mL × 2), and brine. The aqueous extracts were collected and re-extracted with EtOAc (50 mL × 4). The organic extracts were collected, dried over anhydrous Na_2SO_4, and chromatographed (SiO_2, 80% EtOAc/hexane) to afford 8 mg of compound **5** (16.5%, colorless amorphous powder) and 13 mg of compound **6** (25%, white amorphous powder).

3-*O*-Acetyl bruceine C (**5**): ^{1}H NMR (270 MHz, $CDCl_3$) δ 6.26 (1H, br s, H-15), 6.07 (1H, d, J = 1.3 Hz, H-2′), 4.78 (1H, s, H-7), 4.73 (1H, d, J = 8.1 Hz, H_a-20), 4.26 (1H, m, H-11), 4.18 (1H, s, H-12), 3.79 (1H, d, J = 8.1 Hz, H_b-20), 3.76 (3H, s, OCH_3), 3.15 (1H, br s, H-14), 3.09 (1H, br d, J = 12.4 Hz, H-5), 2.97 (1H, d, J = 16.2 Hz, H_β-1), 2.46 (1H, d, J = 16.2 Hz, H_α-1), 2.42 (1H, dt, J = 15.0, 3.0 Hz, H_α-6), 2.24 (3H, s, $OCOCH_3$), 2.17 (3H, d, J = 1.1 Hz, H-5′), 2.02 (1H, br s, H-9), 1.86 (1H, m, H_β-6), 1.78 (3H, d, J = 1.3 Hz, H-18), 1.47 (3H, s, H-19), 1.35 (6H, s, H-6′,7′); ^{13}C NMR (67.5 MHz, $CDCl_3$) δ 189.3 (C-2), 171.8 (C-21), 168.7 ($OCOCH_3$), 168.3 (C-16), 167.0 (C-1′), 165.2 (C-3′), 145.5 (C-3), 142.2 (C-4), 111.2 (C-2′), 82.2 (C-7), 81.3 (C-13), 75.7 (C-4′), 74.2 (C-20), 74.0 (C-12), 70.9 (C-11), 65.8 (C-15), 53.1 (OCH_3), 50.9 (C-14), 50.0 (C-1), 45.3 (C-8), 42.7 (C-5), 41.6 (C-9), 40.7 (C-10), 28.8 (C-6), 28.4 (C-6′,7′), 20.2 ($OCOCH_3$), 15.7 (C-19), 15.4 (C-5′), 14.5 (C-18); HRFABMS m/z 605.2240 $[M - H]^-$ (calcd for $C_{30}H_{37}O_{13}$, 605.2234).

3,12-Di-*O*-acetyl bruceine C (**6**): ^{1}H NMR (270 MHz, $CDCl_3$) δ 6.05 (1H, d, J = 1.3 Hz, H-2′), 5.27 (1H, s, H-12), 4.79 (1H, s, H-7), 4.76 (1H, d, J = 7.6 Hz, H_a-20), 4.11 (1H, m, H-11), 3.79 (1H, d, J = 7.6 Hz, H_b-20), 3.71 (3H, s, OCH_3), 3.30 (1H, br d, J = 13.5 Hz, H-14), 3.08 (1H, br d, J = 12.2 Hz, H-5), 2.92 (1H, d, J = 16.2 Hz, H_β-1), 2.40 (1H, d, J = 16.2 Hz, H_α-1), 2.35 (1H, m, H_α-6), 2.23 (3H, s, $OCOCH_3$), 2.15 (3H, d, J = 1.1 Hz, H-5′), 2.02 (1H, br s, H-9), 1.99 (3H, s, $OCOCH_3$), 1.82 (1H, m, H_β-6), 1.78 (3H, d, J = 1.3 Hz, H-18), 1.46 (3H, s, H-19), 1.35 (3H, s, H-6′), 1.34 (3H, s, H-7′); ^{13}C NMR (67.5 MHz, $CDCl_3$) δ 189.2 (C-2), 169.3 (C-21), 168.9 ($OCOCH_3$), 168.7 ($OCOCH_3$), 168.4 (C-16), 167.1 (C-1′), 165.2 (C-3′), 145.7 (C-3), 142.2 (C-4), 111.2 (C-2′), 82.6 (C-7), 80.4 (C-13), 74.3 (C-4′), 74.1 (C-20), 74.0 (C-12), 69.4 (C-11), 65.5 (C-15), 52.9 (OCH_3), 50.9 (C-14), 49.9 (C-1), 44.9 (C-8), 42.7 (C-5), 42.1 (C-9), 40.6 (C-10), 28.8 (C-6), 28.4 (C-6′), 28.3 (C-7′), 20.7 ($OCOCH_3$), 20.2 ($OCOCH_3$), 15.5 (C-19), 15.4 (C-5′), 14.5 (C-18); HRFABMS m/z 647.2325 $[M - H]^-$ (calcd for $C_{32}H_{39}O_{14}$, 647.2340).

*3-O-t-Butyl dimethylsilyl-bruceine C (**7**)*

Tert-butyl(chloro)dimethylsilane (93.75 mg, 0.625 mmol) and imidazole (127.5 mg, 1.875 mmol) were added to a solution of bruceine C (**2**) (75 mg, 0.13 mmol) in *N*,*N*-dimethylformamide (0.75 mL), and the mixture was stirred at room temperature under a nitrogen atmosphere for 24 h. The reaction mixture was dissolved in EtOAc (30 mL) and washed with 0.1 M HCl (20 mL × 2), $NaHCO_3$ (20 mL × 2), and brine. The aqueous extracts were collected and re-extracted with EtOAc (50 mL × 4). The organic extracts were collected, dried over anhydrous Na_2SO_4, and chromatographed (SiO_2, 80% EtOAc/hexane) to afford 60 mg of compound **7** (68%, colorless amorphous solid).

^{1}H NMR (270 MHz, $CDCl_3$) δ 6.25 (1H, br s, H-15), 6.06 (1H, d, J = 1.3 Hz, H-2′), 4.77 (1H, s, H-7), 4.72 (1H, d, J = 8.1 Hz, H_a-20), 4.24 (1H, m, H-11), 4.17 (1H, s, H-12), 3.78 (1H, d, J = 8.1 Hz, H_b-20), 3.75 (3H, s, OCH_3), 3.15 (1H, br d, J = 11.9 Hz, H-14), 2.96 (1H, br d, J = 12.9 Hz, H-5), 2.89 (1H, d, J = 15.7 Hz, H_β-1), 2.40 (1H, d, J = 15.7 Hz, H_α-1), 2.33 (1H, m, H_α-6), 2.16 (3H, d, J = 1.1 Hz, H-5′), 2.02 (1H, br s, H-9), 1.83 (3H, d, J = 1.3 Hz, H-18), 1.79 (1H, m, H_β-6), 1.36 (3H, s, H-19), 1.35 (6H, s, H-6′,7′), 0.93 (9H, s, Me_3CSi), 0.15 and 0.11 (3H each, s, Me_2Si); ^{13}C NMR (67.5 MHz, $CDCl_3$) δ 192.2

(C-2), 171.8 (C-21), 168.2 (C-16), 167.1 (C-1′), 165.2 (C-3′), 145.1 (C-3), 136.2 (C-4), 111.3 (C-2′), 82.6 (C-7), 81.4 (C-13), 75.7 (C-4′), 74.2 (C-20), 74.1 (C-12), 71.0 (C-11), 66.0 (C-15), 53.1 (OCH_3), 51.6 (C-14), 50.5 (C-1), 45.3 (C-8), 42.5 (C-5), 41.7 (C-9), 40.3 (C-10), 29.3 (C-6), 28.4 (C-6′,7′), 26.0 (Me_3CSi, 3C), 18.8 (Me_3CSi), 15.7 (C-19), 15.5 (C-5′), 14.4 (C-18), −3.8, −4.0 (Me_2Si); HRFABMS *m/z* 679.3176 $[M + H]^+$ (calcd for $C_{34}H_{51}O_{12}Si$, 679.3150).

*3-O-t-Butyl dimethylsilyl-11,12-di-O-acetyl bruceine C (**8**)*

Acetic anhydride (20 μL, 0.2 mmol) was added to a solution of compound **7** (60 mg, 0.088 mmol), a catalytic amount of DMAP (15 mg, 0.12 mmol), and pyridine (0.2 mL) in CH_2Cl_2 (2.0 mL). After being stirred at room temperature for 20 h, the reaction mixture was dissolved in EtOAc (30 mL) and washed with 1 M HCl (20 mL × 3), $NaHCO_3$ (20 mL × 2), and brine. The aqueous extracts were collected and re-extracted with EtOAc (50 mL × 4). The organic extracts were collected, dried over anhydrous Na_2SO_4, and chromatographed (SiO_2, 70% EtOAc/hexane), to afford 34 mg of compound **8** (50.7%, colorless amorphous powder).

^1H NMR (270 MHz, $CDCl_3$) δ 6.12 (1H, br s, H-15), 6.02 (1H, d, J = 1.1 Hz, H-2′), 5.27 (1H, s, H-12), 5.20 (1H, d, J = 4.9 Hz, H-11), 4.79 (1H, s, H-7), 4.73 (1H, d, J = 7.7 Hz, H_a-20), 3.83 (1H, d, J = 7.7 Hz, H_b-20), 3.67 (3H, s, OCH_3), 3.23 (1H, br d, J = 12.4 Hz, H-14), 3.05 (1H, br d, J = 12.7 Hz, H-5), 2.53 (1H, d, J = 16.1 Hz, H_β-1), 2.42 (1H, m, H_α-6), 2.35 (1H, d, J = 16.1 Hz, H_α-1), 2.15 (3H, d, J = 1.1, H-5′), 2.08 (3H, s, $OCOCH_3$), 2.02 (1H, br s, H-9), 2.01 (3H, s, $OCOCH_3$), 1.85 (3H, d, J = 1.6 Hz, H-18), 1.74 (1H, m, H_β-6), 1.35 (3H, s, H-6′), 1.32 (3H, s, H-7′), 1.15 (3H, s, H-19), 0.92 (9H, s, Me_3CSi), 0.15 and 0.07 (3H each, s, Me_2Si); ^{13}C NMR (67.5 MHz, $CDCl_3$) δ 191.3 (C-2), 168.9 (C-21), 168.5 ($OCOCH_3$, 2C), 167.8 (C-16), 167.0 (C-1′), 165.2 (C-3′), 144.8 (C-3), 136.4 (C-4), 111.2 (C-2′), 82.7 (C-7), 79.9 (C-13), 74.0 (C-4′), 73.8 (C-20), 70.8 (C-12), 69.1 (C-11), 65.4 (C-15), 52.9 (OCH_3), 51.6 (C-14), 50.5 (C-1), 44.9 (C-8), 42.4 (C-5), 41.1 (C-9), 39.7 (C-10), 29.0 (C-6), 28.4 (C-6′), 28.3 (C-7′), 26.0 (Me_3CSi, 3C), 21.5 ($OCOCH_3$), 20.7 ($OCOCH_3$), 18.8 (Me_3CSi), 15.6 (C-19), 15.5 (C-5′), 14.5 (C-18), −3.7, −4.1 (Me_2Si); HRFABMS *m/z* 763.3348 $[M + H]^+$ (calcd for $C_{38}H_{55}O_{14}Si$, 763.3361).

*11,12-Di-O-acetyl bruceine C (**9**)*

A tetrabutylammonium fluoride solution (1.0 M in tetrahydrofuran, 120 μL, 0.120 mmol) was added to a solution of **8** (18 mg, 0.024 mmol) in tetrahydrofuran (0.5 mL), and the mixture was stirred at room temperature under a nitrogen atmosphere for 15 min. The mixture was diluted with chloroform (30 mL), washed sequentially with water (10 mL) and brine (10 mL), dried over anhydrous Na_2SO_4, and filtered. The solvent was removed in vacuo, and the crude product was chromatographed (SiO_2, 80% EtOAc/hexane) to afford 4 mg of compound **9** (25.7%, colorless amorphous solid).

^1H NMR (500 MHz, $CDCl_3$) δ 6.07 (1H, d, J = 1.0 Hz, H-2′), 6.06 (1H, br s, H-15), 5.29 (1H, s, H-12), 5.21 (1H, d, J = 4.0 Hz, H-11), 4.82 (1H, s, H-7), 4.74 (1H, d, J = 8.0 Hz, H_a-20), 3.84 (1H, d, J = 8.0 Hz, H_b-20), 3.70 (3H, s, OCH_3), 3.26 (1H, br d, J = 13.5 Hz, H-14), 2.99 (1H, br d, J = 12.5 Hz, H-5), 2.65 (1H, d, J = 16.0 Hz, H_β-1), 2.42 (1H, dt, J = 15.0, 3.0 Hz, H_α-6), 2.34 (1H, d, J = 16.0 Hz, H_α-1), 2.17 (3H, d, J = 1.0 Hz, H-5′), 2.10 (3H, s, $OCOCH_3$) 2.03 (1H, br s, H-9), 2.02 (3H, s, $OCOCH_3$), 1.84 (3H, d, J = 2.0 Hz, H-18), 1.75 (1H, ddd, J = 15.0, 13.0, 2.5 Hz, H_β-6), 1.37 (3H, s, H-6′), 1.35 (3H, s, H-7′), 1.18 (3H, s, H-19); ^{13}C NMR (125 MHz, $CDCl_3$) δ 190.9 (C-2), 168.8 (C-21), 168.6 ($OCOCH_3$), 168.3 ($OCOCH_3$), 167.7 (C-16), 166.8 (C-1′), 165.1 (C-3′), 144.0 (C-3), 127.4 (C-4), 111.2 (C-2′), 82.6 (C-7), 79.9 (C-13), 74.2 (C-4′), 73.7 (C-20), 70.9 (C-12), 69.1 (C-11), 52.9 (OCH_3), 48.7 (C-1), 45.1 (C-8), 42.0 (C-5), 41.5 (C-9), 40.6 (C-10), 28.9 (C-6), 28.5 (C-6′), 28.5 (C-7′), 21.5 ($OCOCH_3$), 20.6 ($OCOCH_3$), 15.5 (C-19), 15.5 (C-5′), 13.3 (C-18); HRFABMS *m/z* 647.2360 $[M - H]^-$ (calcd for $C_{32}H_{39}O_{14}$, 647.2340).

*3-O-Acetyl bruceantinol (3,4′-di-O-acetyl bruceine C, **10**)*

Acetic anhydride (10 μL, 0.1 mmol) was added to a solution of bruceantinol (**3**) (45 mg, 0.08 mmol), a catalytic amount of DMAP (15 mg, 0.12 mmol), and pyridine (0.2 mL) in CH_2Cl_2 (2.0 mL). After being stirred at room temperature for 20 h, the reaction mixture was dissolved in EtOAc (30 mL) and washed with 1 M HCl (20 mL × 3), $NaHCO_3$ (20 mL × 2), and brine. The aqueous extracts were collected and re-extracted with EtOAc (50 mL × 4). The organic extracts were collected, dried over anhydrous Na_2SO_4, and chromatographed (SiO_2, 80% EtOAc/hexane) to afford 10 mg of compound **10** (22%, colorless amorphous powder).

^1H NMR (270 MHz, $CDCl_3$) δ 6.21 (1H, br s, H-15), 5.75 (1H, d, J = 1.1 Hz, H-2′), 4.80 (1H, s, H-7), 4.73 (1H, d, J = 8.1 Hz, H_a-20), 4.24 (1H, m, H-11), 4.19 (1H, s, H-12), 3.82 (1H, d, J = 8.1 Hz, H_b-20), 3.79 (3H, s, OCH_3), 3.19 (1H, br d, J = 11.6 Hz, H-14), 3.06 (1H, br d, J = 13.2 Hz, H-5), 3.00 (1H, d, J = 16.2 Hz, H_β-1), 2.43 (1H, d, J = 16.2 Hz, H_α-1), 2.36 (1H, m, H_α-6), 2.24 (3H, s, $OCOCH_3$), 2.12 (3H, d, J = 1.1 Hz, H-5′), 2.01 (1H, br s, H-9), 2.00 (3H, s, $OCOCH_3$), 1.81 (1H, m, H_β-6), 1.78 (3H, d, J = 1.3 Hz, H-18), 1.51 (3H, s, H-6′), 1.49 (3H, s,

H-7′), 1.48 (3H, s, H-19); ^{13}C NMR (67.5 MHz, $CDCl_3$) δ 189.0 (C-2), 171.7 (C-21), 169.6 ($OCOCH_3$), 168.7 ($OCOCH_3$), 166.8 (C-16), 165.6 (C-1′), 164.7 (C-3′), 145.1 (C-3), 142.3 (C-4), 111.7 (C-2′), 82.2 (C-4′), 82.1 (C-7), 81.2 (C-13), 75.7 (C-20), 73.9 (C-12), 70.9 (C-11), 66.2 (C-15), 53.3 (OCH_3), 50.9 (C-14), 50.1 (C-1), 45.3 (C-8), 42.8 (C-5), 41.7 (C-9), 40.7 (C-10), 28.9 (C-6), 26.3 (C-6′), 26.1 (C-7′), 21.6 ($OCOCH_3$), 20.2 ($OCOCH_3$), 15.5 (C-19), 14.6 (C-18), 14.5 (C-5′); HRFABMS *m/z* 647.2331 $[M - H]^-$ (calcd for $C_{32}H_{39}O_{14}$, 647.2340).

*3,11,12-Tri-O-acetyl bruceine A (**11**)*

Acetic anhydride (0.5 mL, 5.0 mmol) was added to a solution of bruceine A (**1**) (33 mg, 0.063 mmol), a catalytic amount of DMAP (15 mg, 0.12 mmol), and pyridine (0.5 mL) in CH_2Cl_2 (2.0 mL). After being stirred at room temperature for 20 h, the reaction mixture was dissolved in EtOAc (30 mL) and washed with 1 M HCl (20 mL × 3), $NaHCO_3$ (20 mL × 2), and brine. The aqueous extracts were collected and re-extracted with EtOAc (50 mL × 4). The organic extracts were collected, dried over anhydrous Na_2SO_4, and chromatographed (SiO_2, 60% EtOAc/hexane) to afford 30 mg of compound **11** (73%, white amorphous powder).

^{1}H NMR (270 MHz, $CDCl_3$) δ 6.08 (1H, br s, H-15), 5.29 (1H, s, H-12), 5.20 (1H, d, J = 5.1 Hz, H-11), 4.81(1H, s, H-7), 4.74 (1H, d, J = 7.5 Hz, H_a-20), 3.82 (1H, d, J = 7.5 Hz, H_b-20), 3.79 (3H, s, OCH_3), 3.24 (1H, br d, J = 13.2 Hz, H-14), 3.06 (1H, br d, J = 12.7 Hz, H-5), 2.64 (1H, d, J = 16.3 Hz, H_β-1), 2.42 (1H, dt, J = 15.0, 3.0 Hz, H_α-6), 2.38 (1H, d, J = 16.3 Hz, H_α-1), 2.23 (3H, s, $OCOCH_3$), 2.22 (1H, d, J = 8.1 Hz, H_a-2′), 2.19 (1H, d, J = 6.6 Hz, H_b-2′), 2.10 (3H, s, $OCOCH_3$), 2.08 (1H, m, H-3′), 2.06 (1H, br s, H-9), 2.02 (3H, s, $OCOCH_3$), 1.83 (1H, m, H_β-6), 1.78 (3H, d, J = 1.1 Hz, H-18), 1.28 (3H, s, H-19), 0.97 (3H, d, J = 6.6 Hz, H-4′), 0.96 (3H, d, J = 6.6 Hz, H-5′); ^{13}C NMR (67.5 MHz, $CDCl_3$) δ 187.8 (C-2), 171.3 (C-21), 168.7 ($OCOCH_3$), 168.7 ($OCOCH_3$), 168.5 ($OCOCH_3$), 167.6 (C-16), 166.4 (C-1′), 144.7 (C-3), 142.3 (C-4), 82.2 (C-7), 79.8 (C-13), 73.5 (C-20), 70.8 (C-12), 69.0 (C-11), 65.7 (C-15), 52.9 (OCH_3), 51.2 (C-14), 50.1 (C-1), 45.0 (C-8), 42.8 (C-5), 42.7 (C-2′), 41.2 (C-9), 40.2 (C-10), 28.6 (C-6), 25.4 (C-3′), 22.4 (C-4′,5′), 21.4 ($OCOCH_3$), 20.7 ($OCOCH_3$), 20.2 ($OCOCH_3$), 15.6 (C-19), 14.5 (C-18); HRFDMS *m/z* 648.2386 $[M]^+$ (calcd for $C_{32}H_{40}O_{14}$, 648.2418).

*3-O-Acetyl bruceine A (**12**)*

Acetic anhydride (10 μL, 0.1 mmol) was added to a solution of bruceine A (**1**) (50 mg, 0.096 mmol), a catalytic amount of DMAP (15 mg, 0.12 mmol), and pyridine (0.5 mL) in CH_2Cl_2 (2.0 mL). After being stirred at room temperature for 20 h, the reaction mixture was dissolved in EtOAc (30 mL) and washed with 1 M HCl (20 mL × 3), $NaHCO_3$ (20 mL × 2), and brine. The aqueous extracts were collected and re-extracted with EtOAc (50 mL × 4). The organic extracts were collected, dried over anhydrous $MgSO_4$, and chromatographed (SiO_2, 70% EtOAc/hexane), to afford 46 mg of compound **12** (85%, white amorphous powder).

^{1}H NMR (270 MHz, $CDCl_3$) δ 6.30 (1H, br d, J = 12.2 Hz, H-15), 4.74 (1H, s, H-7), 4.72 (1H, d, J = 8.1 Hz, H_a-20), 4.22 (1H, m, H-11), 4.16 (1H, s, H-12), 3.80 (3H, s, OCH_3), 3.76 (1H, d, J = 8.1 Hz, H_b-20), 3.36 (1H, m, H-14), 3.05 (1H, br d, J = 11.3 Hz, H-5), 2.96 (1H, d, J = 16.2 Hz, H_β-1), 2.45 (1H, d, J = 16.2 Hz, H_α-1), 2.38 (1H, dt, J = 15.0, 3.0 Hz, H_α-6), 2.23 (3H, s, $OCOCH_3$), 2.18 (1H, br s, H-9), 2.15 (1H, d, J = 7.6 Hz, H_a-2′), 2.12 (1H, d, J = 6.6 Hz, H_b-2′), 2.07 (1H, m, H-3′), 1.86 (1H, m, H_β-6), 1.77 (3H, d, J = 1.1 Hz, H-18), 1.45 (3H, s, H-19), 0.96 (6H, d, J = 6.6 Hz, H-4′,5′); ^{13}C NMR (67.5 MHz, $CDCl_3$) δ 189.4 (C-2), 171.9 (C-21), 171.3 ($OCOCH_3$), 168.8 (C-16), 166.7 (C-1′), 145.5 (C-3), 142.2 (C-4), 82.3 (C-7), 81.2 (C-13), 73.8 (C-20), 70.9 (C-12), 70.8 (C-11), 66.2 (C-15), 53.0 (OCH_3), 51.4 (C-14), 49.9 (C-1), 45.3 (C-8), 42.8 (C-5), 42.6 (C-2′), 41.7 (C-9), 40.7 (C-10), 28.8 (C-6), 25.4 (C-3′), 22.4 (C-4′,5′), 20.2 ($OCOCH_3$), 15.5 (C-19), 14.5 (C-18); HRFDMS *m/z* 564.21799 $[M]^+$ (calcd for $C_{28}H_{36}O_{12}$, 564.22068).

*3,12-Di-O-acetyl bruceine A (**13**)*

Acetic anhydride (5 μL, 0.05 mmol) was added to a solution of compound (**12**) (28 mg, 0.05 mmol), a catalytic amount of DMAP (15 mg, 0.12 mmol), and pyridine (0.2 mL) in CH_2Cl_2 (2.0 mL). After being stirred at room temperature for 20 h, the reaction mixture was dissolved in EtOAc (30 mL) and washed with 1 M HCl (20 mL × 3), $NaHCO_3$ (20 mL × 2), and brine. The aqueous extracts were collected and re-extracted with EtOAc (50 mL × 4). The organic extracts were collected, dried over anhydrous Na_2SO_4, and chromatographed (SiO_2, 70% EtOAc/hexane) to afford 7 mg of compound **13** (23%, white amorphous powder).

^{1}H NMR (500 MHz, $CDCl_3$) δ 6.04 (1H, br s, H-15), 5.28 (1H, s, H-12), 4.77 (1H, s, H-7), 4.75 (1H, d, J = 7.5 Hz, H_a-20), 4.11 (1H, m, H-11), 3.77 (1H, d, J = 7.5 Hz, H_b-20), 3.76 (3H, s, OCH_3), 3.25 (1H, br d, J = 12.5 Hz, H-14), 3.02 (1H, br d, J = 13.0 Hz, H-5), 2.94 (1H, d, J = 16.0 Hz, H_β-1), 2.39 (1H, d, J = 16.0 Hz, H_α-1), 2.38 (1H, m, H_α-6), 2.24 (3H, s, $OCOCH_3$), 2.22 (1H, d, J = 7.0 Hz, H_a-2′), 2.19 (1H, d, J = 7.0 Hz, H_b-2′), 2.12 (1H, m, H-3′), 2.01 (3H, s, $OCOCH_3$), 1.86 (1H, ddd, J = 15.5, 12.5, 3.0 Hz, H_β-6), 1.78 (3H, d,

J = 1.5 Hz, H-18), 1.47 (3H, s, H-19), 0.97 (3H, d, J = 6.5 Hz, H-4′), 0.96 (3H, d, J = 6.5 Hz, H-5′); ^{13}C NMR (67.5 MHz, $CDCl_3$) δ 188.7 (C-2), 171.3 (C-21), 169.1 ($OCOCH_3$), 168.7 ($OCOCH_3$), 168.7 (C-16), 166.5 (C-1′), 145.0 (C-3), 142.3 (C-4), 82.4 (C-7), 80.4 (C-13), 74.4 (C-12), 73.6 (C-20), 69.5 (C-11), 65.7 (C-15), 52.9 (OCH_3), 51.0 (C-14), 50.0 (C-1), 45.0 (C-8), 42.8 (C-5), 42.8 (C-2′), 42.3 (C-9), 40.7 (C-10), 28.8 (C-6), 25.5 (C-3′), 22.4 (C-4′,5′), 20.7 ($OCOCH_3$), 20.2 ($OCOCH_3$), 15.5 (C-19), 14.5 (C-18); HRFDMS m/z 607.23948 $[M + H]^+$ (calcd for $C_{30}H_{39}O_{13}$, 607.23906).

*3-O-t-Butyl dimethylsilyl-bruceine A (**14**)*

Tert-butyl(chloro)dimethylsilane (93.75 mg, 0.625 mmol) and imidazole (127.5 mg, 1.875 mmol) were added to a solution of bruceine A (**1**) (100 mg, 0.19 mmol) in *N*,*N*-dimethylformamide (1.0 mL), and the mixture was stirred at room temperature under a nitrogen atmosphere for 24 h. The reaction mixture was dissolved in EtOAc (30 mL) and washed with 0.1 M HCl (20 mL × 2), $NaHCO_3$ (20 mL × 2), and brine. The aqueous extracts were collected and re-extracted with EtOAc (50 mL × 4). The organic extracts were collected, dried over anhydrous Na_2SO_4, and chromatographed (SiO_2, 70% EtOAc/hexane) to afford 94 mg of compound **14** (77.8%, colorless amorphous solid).

^{1}H NMR (270 MHz, $CDCl_3$) δ 6.24 (1H, br s, H-15), 4.72 (1H, s, H-7), 4.70 (1H, d, J = 8.1 Hz, H_a-20), 4.23 (1H, m, H-11), 4.18 (1H, s, H-12), 3.79 (3H, s, OCH_3), 3.75 (1H, d, J = 8.1 Hz, H_b-20), 3.07 (1H, br d, J = 12.7 Hz, H-14), 2.92 (1H, br d, J = 12.9 Hz, H-5), 2.87 (1H, d, J = 16.2 Hz, H_β-1), 2.36 (1H, d, J = 16.2 Hz, H_α-1), 2.31 (1H, m, H_α-6), 2.18 (1H, d, J = 6.5 Hz, H_a-2′), 2.15 (1H, d, J = 7.8 Hz, H_b-2′), 2.05 (1H, m, H-3′), 2.02 (1H, br s, H-9), 1.82 (3H, d, J = 1.3 Hz, H-18), 1.78 (1H, ddd, J = 15.1, 13.2, 2.7 Hz, H_β-6), 1.35 (3H, s, H-19), 0.95 (6H, d, J = 6.5 Hz, H-4′,5′), 0.91 (9H, s, Me_3CSi), 0.13 and 0.10 (3H each, s, Me_2Si); ^{13}C NMR (67.5 MHz, $CDCl_3$) δ 192.3 (C-2), 171.7 (C-21), 171.2 (C-16), 166.8 (C-1′), 144.9 (C-3), 136.2 (C-4), 82.6 (C-7), 81.3 (C-13), 75.6 (C-20), 73.8 (C-12), 71.1 (C-11), 66.2 (C-15), 53.0 (OCH_3), 51.4 (C-14), 50.4 (C-1), 45.3 (C-8), 42.6 (C-5), 42.6 (C-2′), 41.8 (C-9), 40.3 (C-10), 29.2 (C-6), 25.9 (Me_3CSi, 3C), 25.4 (C-3′), 22.4 (C-4′), 22.3 (C-5′), 18.7 (Me_3CSi), 15.5 (C-19), 14.4 (C-18), −3.8, −4.0 (Me_2Si); HRFABMS m/z 635.2878 $[M - H]^-$ (calcd for $C_{32}H_{47}O_{11}Si$, 635.2888).

*3-O-t-Butyl dimethylsilyl-12-O-acetyl bruceine A (**15**)*

Acetic anhydride (15 μL, 0.15 mmol) was added to a solution of compound **14** (90 mg, 0.14 mmol), a catalytic amount of DMAP (15 mg, 0.12 mmol), and pyridine (0.5 mL) in CH_2Cl_2 (2.0 mL). After being stirred at room temperature for 20 h, the reaction mixture was dissolved in EtOAc (30 mL) and washed with 1 M HCl (20 mL × 3), $NaHCO_3$ (20 mL × 2), and brine. The aqueous extracts were collected and re-extracted with EtOAc (50 mL × 4). The organic extracts were collected, dried over anhydrous Na_2SO_4, and chromatographed (SiO_2, 50% EtOAc/hexane) to afford 26 mg of compound **15** (27.4%, colorless amorphous powder).

^{1}H NMR (270 MHz, $CDCl_3$) δ 6.05 (1H, br d, J = 9.7 Hz, H-15), 5.28 (1H, s, H-12), 4.75 (1H, s, H-7), 4.72 (1H, d, J = 7.6 Hz, H_a-20), 4.10 (1H, m, H-11), 3.76 (3H, s, OCH_3), 3.74 (1H, d, J = 7.6 Hz, H_b-20), 3.24 (1H, br d, J = 13.5 Hz, H-14), 2.90 (1H, br d, J = 10.5 Hz, H-5), 2.86 (1H, d, J = 15.2 Hz, H_β-1), 2.40 (1H, dt, J = 15.0, 3.0 Hz, H_α-6), 2.28 (1H, d, J = 15.2 Hz, H_α-1), 2.25 (1H, d, J = 7.0 Hz, H_a-2′), 2.17 (1H, d, J = 7.6 Hz, H_b-2′), 2.12 (1H, m, H-3′), 2.02 (1H, br s, H-9), 2.01 (3H, s, $OCOCH_3$), 1.82 (3H, d, J = 1.6 Hz, H-18), 1.76 (1H, ddd, J = 15.0, 13.0, 2.4 Hz, H_β-6), 1.35 (3H, s, H-19), 0.98 (3H, d, J = 6.3 Hz, H-4′), 0.97 (3H, d, J = 6.3 Hz, H-5′), 0.93 (9H, s, Me_3CSi), 0.14 and 0.11 (3H each, s, Me_2Si); ^{13}C NMR (67.5 MHz, $CDCl_3$) δ 191.5 (C-2), 171.4 (C-21), 169.1 ($OCOCH_3$), 168.8 (C-16), 166.6 (C-1′), 145.0 (C-3), 135.5 (C-4), 82.7 (C-7), 80.4 (C-13), 74.0 (C-12), 73.7 (C-20), 69.5 (C-11), 65.8 (C-15), 52.9 (OCH_3), 51.1 (C-14), 50.5 (C-1), 45.0 (C-8), 42.8 (C-5), 42.7 (C-2′), 42.6 (C-9), 40.4 (C-10), 29.3 (C-6), 26.0 (Me_3CSi, 3C), 25.5 (C-3′), 22.4 (C-4′,5′), 20.7 ($OCOCH_3$), 18.8 (Me_3CSi), 15.5 (C-19), 14.4 (C-18), −3.8, −4.0 (Me_2Si); HRFABMS m/z 677.2991 $[M - H]^-$ (calcd for $C_{34}H_{49}O_{12}Si$, 677.2993).

*12-O-Acetyl bruceine A (**16**)*

A tetrabutylammonium fluoride solution (1.0 M in tetrahydrofuran, 180 μL, 0.180 mmol) was added to a solution of **15** (25 mg, 0.036 mmol) in tetrahydrofuran (0.75 mL), and the mixture was stirred at room temperature under a nitrogen atmosphere for 15 min. The mixture was diluted with chloroform (30 mL), washed sequentially with water (10 mL) and brine (10 mL), dried over anhydrous Na_2SO_4, and filtered. The solvent was removed in vacuo, and the crude product was chromatographed (SiO_2, 60% EtOAc/hexane) to afford 13 mg of compound **16** (64%, white amorphous powder).

^{1}H NMR (500 MHz, $CDCl_3$) δ 6.07 (1H, br s, H-15), 5.28 (1H, s, H-12), 4.76 (1H, s, H-7), 4.74 (1H, d, J = 8.0 Hz, H_a-20), 4.08 (1H, m, H-11), 3.77 (1H, d, J = 8.0 Hz, H_b-20), 3.76 (3H, s, OCH_3), 3.24 (1H, br d, J = 12.0 Hz, H-14), 2.93 (1H, d, J = 16.0 Hz, H_β-1), 2.92 (1H, br d, J = 12.0 Hz, H-5), 2.38 (1H, dt, J = 15.0, 3.0 Hz, H_α-6), 2.34 (1H, d, J = 16.0 Hz, H_α-1), 2.31 (1H, br s, H-9), 2.22 (1H, d,

$J = 7.0$ Hz, H_a-2′), 2.18 (1H, d, $J = 7.0$ Hz, H_b-2′), 2.07 (1H, m, H-3′), 2.01 (3H, s, $OCOCH_3$), 1.83 (3H, d, $J = 1.5$ Hz, H-18), 1.79 ((1H, ddd, $J = 15.0$, 13.0, 2.5 Hz, H_β-6), 1.37 (3H, s, H-19), 0.97 (3H, d, $J = 6.8$ Hz, H-4′), 0.96 (3H, d, $J = 6.8$ Hz, H-5′); ^{13}C NMR (67.5 MHz, $CDCl_3$) δ 191.7 (C-2), 171.4 (C-21), 169.2 ($OCOCH_3$), 168.7 (C-16), 166.6 (C-1′), 144.0 (C-3), 127.6 (C-4), 82.6 (C-7), 80.4 (C-13), 74.4 (C-12), 73.7 (C-20), 69.5 (C-11), 65.8 (C-15), 52.9 (OCH_3), 51.1 (C-14), 48.5 (C-1), 45.1 (C-8), 42.8 (C-5), 42.4 (C-2′), 41.8 (C-9), 41.1 (C-10), 29.0 (C-6), 25.5 (C-3′), 22.4 (C-4′,5′), 20.7 ($OCOCH_3$), 15.4 (C-19), 13.3 (C-18); HRFDMS *m/z* 564.22158 $[M]^+$ (calcd for $C_{28}H_{36}O_{12}$, 564.22068).

Acknowledgments The authors are grateful to Mr. Yusuke Takata and Dr. Eri Fukushi (GC–MS and NMR Laboratory, Hokkaido University, Japan) for measuring the mass spectra. Financial support and a postdoctoral fellowship (to Ahmed Elkhateeb) from the Japan Society for the Promotion of Science are highly appreciated.

References

1. Luckins AG (1998) *Trypanosoma evansi* in Asia. Parasitol Today 4:137–142
2. Powar RM, Shegokar VR, Joshi PP, Dani VS, Tankhiwale NS, Truc P, Jannin J, Bhargava A (2006) A rare case of human trypanosomiasis caused by *Trypanosoma evansi*. Indian J Med Microbiol 24:72–74
3. Kibona SN, Matemba L, Kaboya JS, Lubega GW (2006) Drug resistance of *Trypanosoma b rhodesiense* isolates from Tanzania. Trop Med Int Health 11:144–155
4. Lee KH, Hayashi N, Okano M, Nozaki H, Ju-ichi M (1984) Antitumor agents, 65. Brusatol and cleomiscosin-A, antileukemic principles from *Brucea javanica*. J Nat Prod 47:550–551
5. Pavanand K, Nutakul W, Dechatiwongse T, Yoshihira K, Yongvanitchit K, Scovill JP, Flippen-Anderson JL, Gilardi R, George C, Kanchanapee P, Webster HK (1986) In vitro antimalarial activity of *Brucea javanica* against multi-drug resistant *Plasmodium falciparum*. Planta Med 52:108–111
6. Bawm S, Matsuura H, Elkhateeb A, Nabeta K, Subeki, Nonaka N, Oku Y, Katakura K (2008) In vitro antitrypanosomal activities of quassinoid compounds from the fruits of a medicinal plant, *Brucea javanica*. Vet Parasitol 158:288–294
7. Hitotsuyanagi Y, Kim IH, Hasuda T, Yamauchi Y, Takeya K (2006) A structure–activity relationship study of brusatol, an antitumor quassinoid. Tetrahedron 62:4262–4271
8. Murakami N, Umezome T, Mahmud T, Sugimoto M, Kobayashi M, Wataya Y, Kim HS (1998) Anti-malarial activities of acylated bruceolide derivatives. Bioorg Med Chem Lett 8:459–462

Traffic 2011; 12: 1383–1393

doi:10.1111/j.1600-0854.2011.01247.x

The Role of VAMP7/TI-VAMP in Cell Polarity and Lysosomal Exocytosis *in vivo*

Mahito Sato[1,2], Shinichiro Yoshimura[3], Rika Hirai[1], Ayako Goto[3], Masataka Kunii[1,3], Nur Atik[3], Takashi Sato[1], Ken Sato[1], Reiko Harada[3,4], Junko Shimada[5], Toshimitsu Hatabu[5], Hiroshi Yorifuji[2,*] and Akihiro Harada[1,3,*]

[1]Department of Cellular and Molecular Biology, Laboratory for Molecular Traffic, Institute for Molecular and Cellular Regulation, Gunma University, Maebashi 371-8512, Japan
[2]Department of Anatomy, Graduate School of Medicine, Gunma University, Maebashi 371-8511, Japan
[3]Department of Cell Biology, Graduate School of Medicine, Osaka University, Suita 565-0871, Japan
[4]Department of Judo Therapy, Takarazuka University of Medical and Health Care, Takarazuka 666-0162, Japan
[5]School of Health Sciences, Gunma University, Maebashi 371-8511, Japan
**Corresponding authors: Akihiro Harada, aharada@acb.med.osaka-u.ac.jp and Hiroshi Yorifuji, yorifuji@med.gunma-u.ac.jp*

VAMP7 or tetanus neurotoxin-insensitive vesicle-associated membrane protein (TI-VAMP) has been proposed to regulate apical transport in polarized epithelial cells, axonal transport in neurons and lysosomal exocytosis. To investigate the function of VAMP7 *in vivo*, we generated VAMP7 knockout mice. Here, we show that VAMP7 knockout mice are indistinguishable from control mice and display a similar localization of apical proteins in the kidney and small intestine and a similar localization of axonal proteins in the nervous system. Neurite outgrowth of cultured mutant hippocampal neurons was reduced in mutant neurons. However, lysosomal exocytosis was not affected in mutant fibroblasts. Our results show that VAMP7 is required in neurons to extend axons to the full extent. However, VAMP7 does not seem to be required for epithelial cell polarity and lysosomal exocytosis.

Key words: apical transport, axonal outgrowth, cell polarity, knockout mouse, lysosomal exocytosis, SNARE

Received 27 September 2010, revised and accepted for publication 7 July 2011, uncorrected manuscript published online 8 July 2011, published online 5 August 2011

SNARE proteins are known to regulate specific membrane fusion between vesicles and their target membranes (1). SNAREs are therefore thought to ensure the specific distribution of membrane and soluble proteins in various organelles. SNAREs are classified into two groups, i.e. SNAREs on transport vesicles, called v-SNAREs, and those on target membranes, called t-SNAREs. Interactions between v-SNAREs and t-SNAREs lead to the formation of a SNARE complex and mediate the subsequent fusion of vesicles with their appropriate target membrane (1).

VAMP7, also known as TI-VAMP, was previously reported to mediate the fusion of transport vesicles with the apical and axonal plasma membranes (2–4). Several studies have shown that VAMP7 is also localized to the lysosome or the late endosome and is involved in the fusion between these organelles (5). In addition, interactions between VAMP7 and synaptotagmin VII are crucial for Ca^{2+}-regulated lysosomal exocytosis, i.e. the fusion between the plasma membrane and the lysosome (6). Although the cellular functions of VAMP7 have been examined in a variety of cell types in a number of studies, the *in vivo* functions of VAMP7 are still unclear. Thus, to clarify the biological functions of VAMP7, we generated VAMP7 knockout (KO) mice.

We found that VAMP7 deficiency did not display gross abnormality in KO mice. The localization of apical or basolateral markers in epithelial cells was not affected in the kidney and small intestine of KO mice. Lysosomal exocytosis was not affected in mutant fibroblasts. Interestingly, the lengths of axons were reduced in mutant neurons.

Collectively, our results suggest that VAMP7 is required in neurons for axons to fully extend. However, VAMP7 is not necessary for epithelial polarity and lysosomal localization and lysosomal exocytosis.

Results and Discussion

Generation of VAMP7-deficient mice

Since the *VAMP7* gene is located on the X chromosome, the expression of VAMP7 was eliminated in homologous recombinant embryonic stem (ES) cells by a simple gene targeting strategy because ES cells have only one X chromosome. Thus, if VAMP7 were essential for the survival of ES cells, we would not be able to obtain the homologous recombinant cells. To circumvent this problem, we engineered a targeting vector containing partial VAMP7 cDNA sequences (from exons 5 to 8) after the splice acceptor of exon 5 to maintain the expression of VAMP7 in ES cells (Figure 1A). We inserted the internal ribosomal entry site (IRES) sequence and neomycin resistance (*Neo*) gene after the partial VAMP7 cDNA, and these sequences were flanked by two flippase recognition target (FRT) sequences. This cassette, together with exons 3 and 4, can be deleted using the Cre-loxP recombination system (Figure 1A).

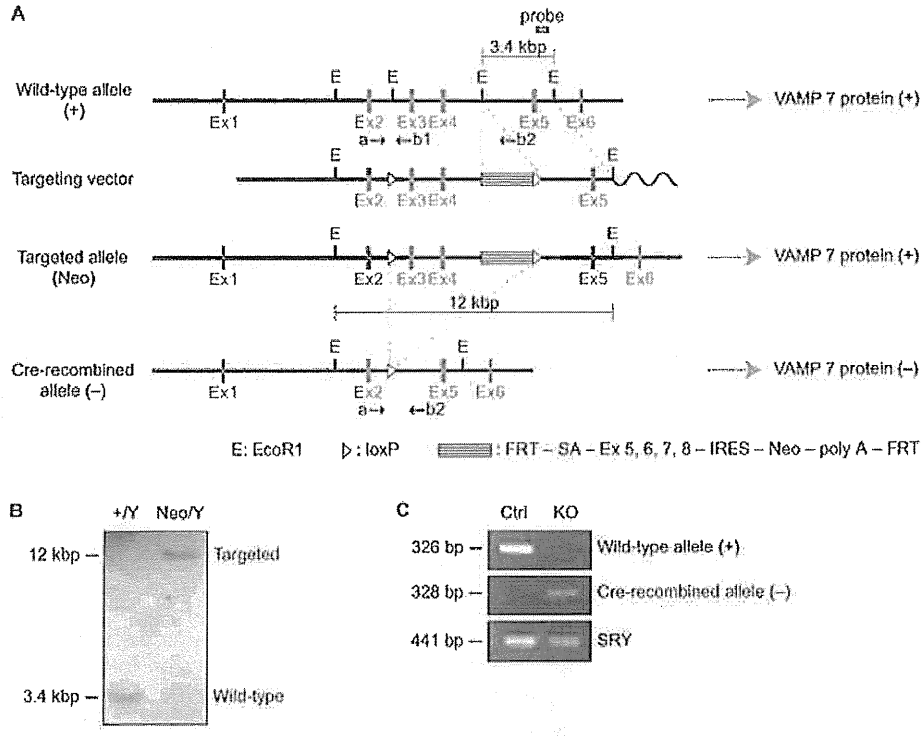

Figure 1: Generation of *VAMP7* KO mice. A) Schematic representation of the wild-type murine *VAMP7* allele (+), the targeting vector, the targeted allele (Neo) and the Cre-recombined *VAMP7* allele (–) obtained after Cre-mediated excision of exons 3 and 4. The wild-type *VAMP7* gene consists of eight coding exons (gray boxes) on chromosome X. In the targeting vector, two loxP sites (white triangles) were introduced into introns flanking exons 3 and 4, and an FRT – splice acceptor (SA) of *VAMP7* exon 5, partial VAMP7 cDNA (exons 5–8), IRES, *Neo*, polyA-FRT cassette – was inserted between exons 4 and 5. In male mice with the Neo resistance gene in an allele of the *VAMP7* gene (Neo/Y), transcription of the *VAMP7* gene is expected to be preserved, because the SA traps the *VAMP7* transcript from exons 1 to 4 and *VAMP7* cDNA (exons 5–8) follows this transcript to produce an intact transcript (exons 1–8). By crossing the Neo/+ mice with transgenic mice that express Cre-recombinase ubiquitously, we generated a *VAMP7* null allele. B) Southern blotting of wild-type (+/Y) and recombinant (Neo/Y) ES cells. Genomic DNAs were digested with *Eco*RI and blotted with the probe indicated in (A). The wild-type allele and the targeted allele generate 3.4- and 12-kb *Eco*RI fragments, respectively. C) PCR analysis of the *VAMP7* alleles of control (Ctrl) and KO mice. To detect the wild-type allele, primers a and b1, indicated in (A), were used. To detect the Cre-recombined allele, primers a and b2 were used. Sex-determining region Y (*SRY*) primers were used for control PCRs.

After electroporation, homologous recombinant ES cells were confirmed by Southern blot analysis (Figure 1B). Heterozygous (+/Neo) female mice were crossed with CMV-Cre mice, which ubiquitously express Cre-recombinase, to obtain VAMP7 KO (–/– or –/Y) mouse lines. KO mice were born at the expected Mendelian frequency. KO mice exhibited no gross abnormality until they died and their life span was similar to the one of control mice. Figure 1C shows a polymerase chain reaction (PCR) analysis of the VAMP7 locus of control (+/Y) and KO (–/Y) mice.

To confirm that the VAMP7 protein was absent in the KO mice, we performed a western blot analysis of several tissues from control and KO mice. As shown in Figure 2A, the VAMP7 protein is highly expressed in the brain, colon, kidney, spleen, stomach, small intestine and lung. Expression of VAMP7 was completely eliminated and no partial proteins were detected in the tissues of KO mice (Figure 2B) with an antibody against exons 5–6. Commercially available antibodies against the N-terminus of VAMP7 did not work in our hands. The loss of VAMP7 protein expression did not lead to markedly increased expression of other SNARE proteins such as VAMP2, 3, 4 and 8 (Figure 2C).

VAMP7 is not essential for the localization of apical and basolateral markers

VAMP7 has been reported to regulate apical transport in epithelial cell lines (3,4). We investigated the effect of VAMP7 disruption on the polarity of epithelial cells from various organs.

Hematoxylin and eosin (HE) staining of the kidney, stomach and small intestine, in which VAMP7 is highly expressed, shows no overt abnormalities in KO mice (Figure 3A). Pocard et al. reported that VAMP7 mediates the direct delivery of both raft- and non-raft-associated apical proteins in a Caco-2 cell, an intestinal cell line (7).

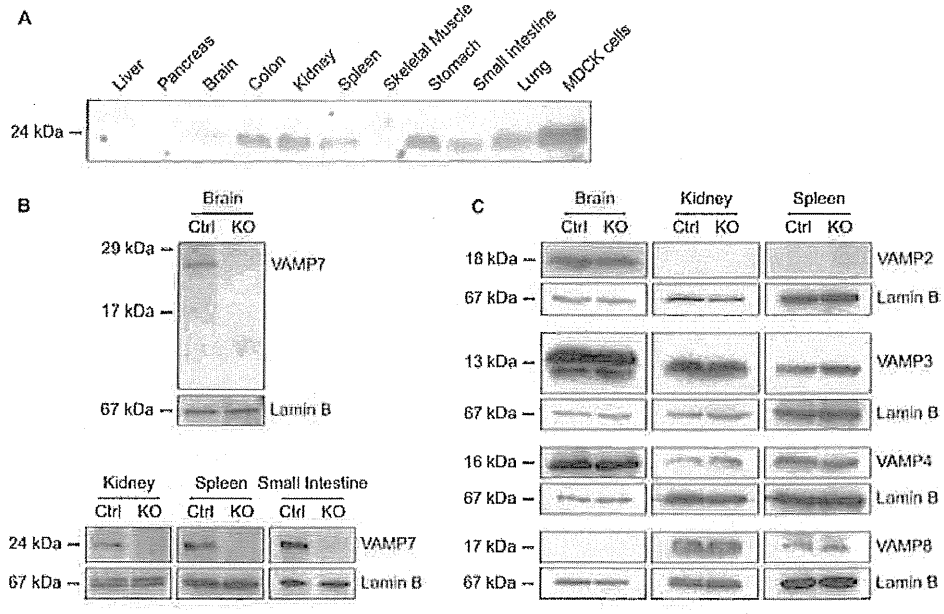

Figure 2: Western blotting of tissues with antibodies against various VAMPs. A) Extracts from various tissues were immunoblotted with anti-VAMP7 rabbit antisera. MDCK cell lysate was loaded as a control. B) Western blot analysis of tissue extracts from control and KO mice with anti-VAMP7, showing no expression of VAMP7 in all KO tissues examined. It also showed the absence of partial smaller protein in a crude extract from KO brain. C) Western blot analysis showing that the levels of other VAMPs (VAMP2, 3, 4 and 8) were similar between the control and KO tissue extracts.

Thus, we investigated the localization of raft- and non-raft-associated apical proteins in the small intestine. As shown in Figure 3B, both alkaline phosphatase (raft-associated) and sodium/glucose cotransporter (SGLT) (non-raft-associated) localized to the apical plasma membrane in the enterocytes of KO mice. E-cadherin, a basolateral marker, localized to the basolateral membrane in the KO enterocytes (Figure 3B). We next examined the localization of apical and basolateral markers in the epithelial cells of renal tubules. The apical markers, dipeptidyl peptidase IV (DPPIV) and SGLT, localize to the apical plasma membrane in the renal epithelial cells of KO mice (Figure 3C). Localization of E-cadherin was also indistinguishable between control and KO renal tubules (Figure 3C).

These results suggest that VAMP7 is not essential for the distribution of apical and basolateral membrane proteins in the kidney or small intestine.

Axonal elongation is impaired by the loss of VAMP7

Several previous studies reported that neurite outgrowth was impaired in cultured rat hippocampal neurons (8) or PC12 cells (2), in which VAMP7 was functionally perturbed by the overexpression of dominant negative forms or RNAi. To assess structural defects in the nervous system of KO mice, we examined sections of the nervous system by light microscopy (Figure 4A). The gross structures of the cerebellum of KO mice were indistinguishable from those of control mice by HE staining. Furthermore, when we stained frozen sections of the hippocampus and cerebellum with an anti-MAP1A antibody, the dendrites of hippocampal pyramidal cells and cerebellar Purkinje cells were indistinguishable between KO and control mice (Figure 4A).

To further examine the role of VAMP7 in axonal outgrowth, we cultured hippocampal neurons and measured the length of axons (which were positive for an axonal marker, phosphorylated neurofilament) 24, 48 and 72 h after plating (8,9) (Figure 4B). For quantitative analysis, we first measured the fraction of neurons at stage 3 of development, which corresponds to the stage of axonal elongation (9). The proportion of KO neurons at stage 3 increased similarly to that of control neurons at all time-points examined (Figure 4C). To analyze the axonal elongation more precisely, we measured the length of axons from neurons 72 h after plating. We identified that the length of axons in KO neurons was shorter by 15% than the one in control neurons [control: $241 \pm 57\%$ (mean $\pm$ SD); KO: $206 \pm 28\%$ (mean $\pm$ SD); $p = 0.019$; Student's *t*-test] (Figure 4D).

These results suggest that VAMP7 is required in neurons to extend axons to their full extent.

Axonal localization of L1 is not reduced by the loss of VAMP7

It has been reported that VAMP7 is involved in the transport of vesicles containing Neuron-glia Cell Adhesion Molecule (NgCAM), a chick homolog of L1 (10), which is

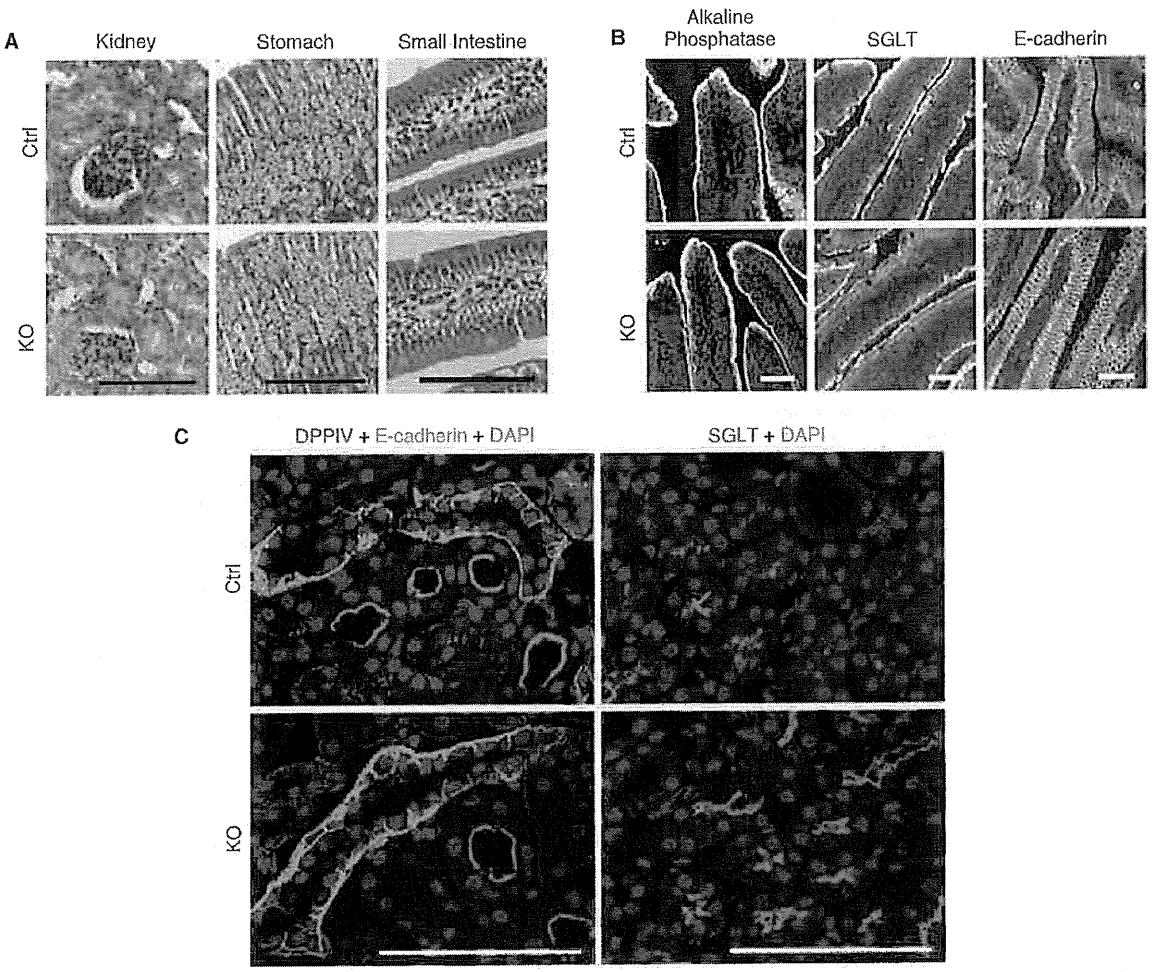

Figure 3: Normal structure and cell polarity of KO epithelial tissues. A) HE-stained paraffin sections from control (Ctrl) and KO mice. B) Localization of apical markers (alkaline phosphatase and SGLT) and a basolateral marker (E-cadherin) in the small intestine. C) Localization of apical markers (DPPIV and SGLT: red) and a basolateral marker (E-cadherin: green) in the kidney. Nuclei were stained by DAPI (blue). Bars, 100 μm.

essential for axonal outgrowth. We therefore expressed NgCAM tagged with green fluorescent protein (NgCAM-GFP) in cultured hippocampal neurons and investigated its distribution. Localization of NgCAM-GFP varied to a great extent from neuron to neuron. However, as shown in Figure 5A, some neurons had localized NgCAM-GFP predominantly in axons. To know the tendency about the localization of NgCAM-GFP between control and KO neurons, we measured the percentage of neurons that had NgCAM-GFP predominantly in axons among all NgCAM-GFP-expressed neurons with discrete axons and dendrites. We did not detect a significant difference in the percentage of neurons, which had NgCAM-GFP in axons rather than dendrites between KO and control neurons [control: 63.3 ± 8.17% (mean ± SD); KO: 61.0 ± 28.4% (mean ± SD); $p = 0.455$; Student's *t*-test]. We further examined the localization of endogenous L1 in KO and control neurons. Staining intensity and localization of L1 were also variable among neurons and it was very difficult to quantitate any trends. However, the localization pattern was similar to NgCAM in both control and KO neurons (Figure 5B).

VAMP7 is not essential for lysosomal distribution

It has been speculated that VAMP7 is involved in lysosomal exocytosis, namely, the fusion of lysosomes to the plasma membrane (11,12). Thus, at the beginning, we examined the distribution and morphology of lysosomes in various tissues of KO mice. As shown in Figure 6A, we found no differences in the distribution or intensity of LAMP2, a lysosomal specific membrane protein, in the kidney or brain between control and KO mice. To examine the morphology of lysosomes and other organelles in more detail, we stained KO and control mouse embryonic fibroblasts (MEFs) with several organelle markers. To differentiate between lysosomes and late endosomes, we

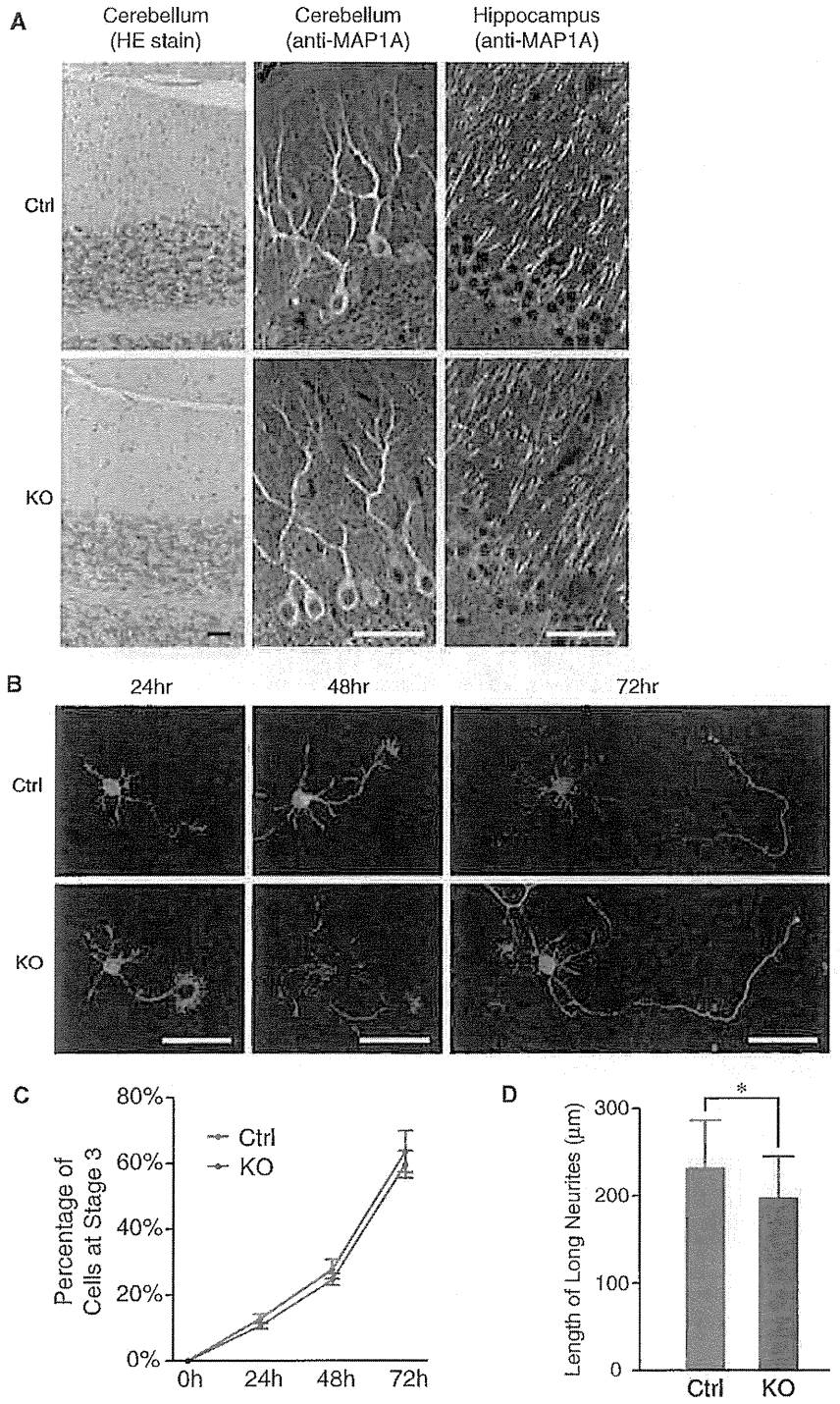

Figure 4: Neuronal architecture and axonal elongation of KO mice. A) HE-stained sagittal sections of cerebellum (left panels), and immunofluorescence micrographs of cerebellum (middle panels) and hippocampus (right panels) stained with an anti-MAP1A antibody. B) Immunofluorescence micrographs of cultured hippocampal neurons 24, 48 and 72 h after plating, showing axonal elongation in both control (Ctrl) and KO cells: phalloidin (green) and phosphorylated neurofilament (red). C) Comparison of the proportions of cultured hippocampal neurons at stage 3 between control (Ctrl) and KO cells, represented as percentiles. The data represent the average ± SD. D) Measurement of the axonal length of cultured hippocampal neurons 72 h after plating between control (Ctrl) and KO cells. The data represent the average ± SD. $*p = 0.019$ Bars, 50 µm.

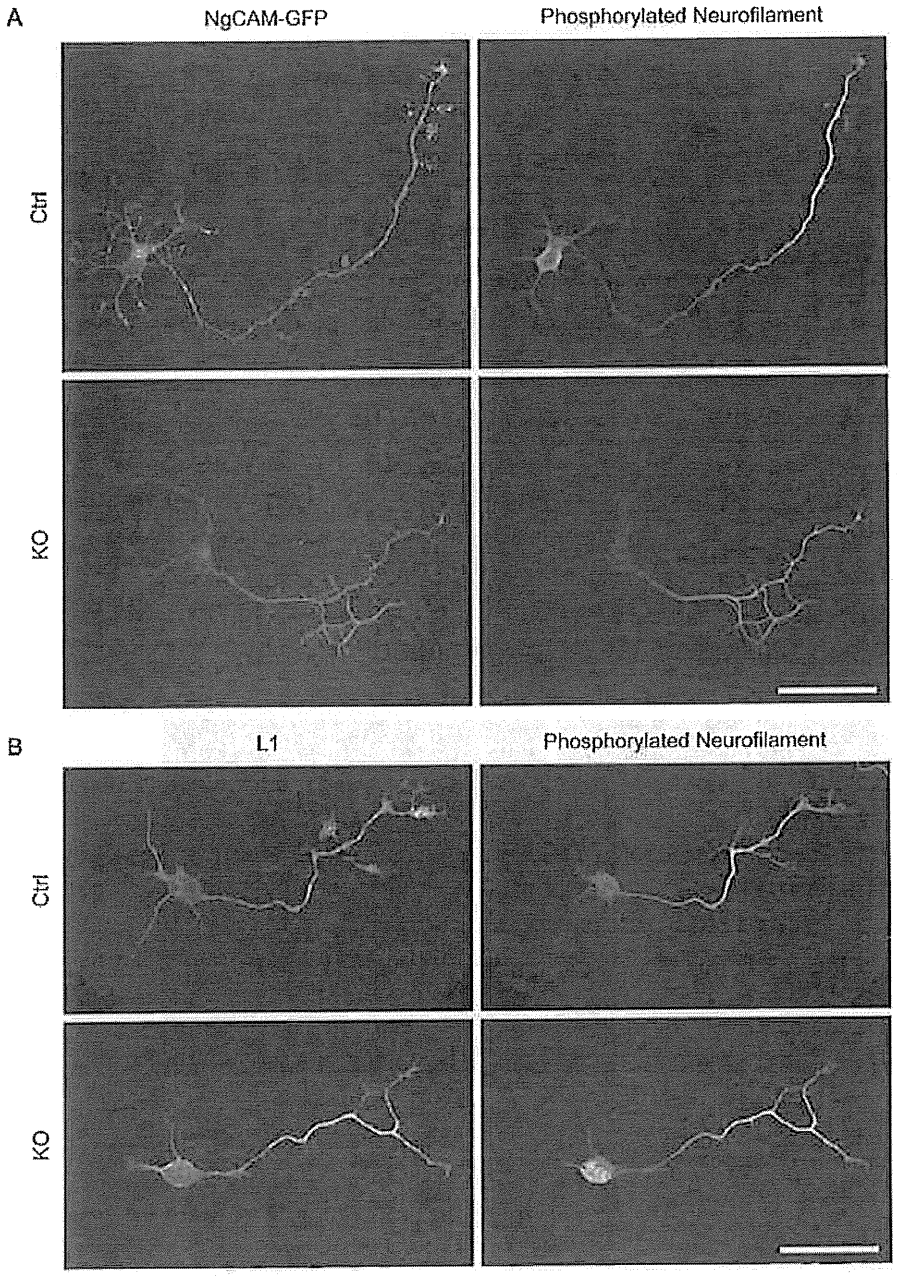

Figure 5: Localization of NgCAM and L1 in the axons. A) Localization of phosphorylated neurofilament and exogenous NgCAM-GFP in control (Ctrl) and KO hippocampal neurons. B) Localization of phosphorylated neurofilament and endogenous L1 in control (Ctrl) and KO hippocampal neurons. Bars, 50 μm.

double-stained the MEFs with lamp2 and other lysosome or late endosome markers (cathepsin D, Rab7 and syntaxin7) and compared their localizations (Figures 6C and S1). We did not find a significant difference in staining in any of these markers. To know the localization and the function of lysosomes further, we simultaneously used LysoTracker and LysoSensor dyes to stain the MEFs (Figure 6C, bottom right). LysoSensor exhibits a pH-dependent increase in fluorescence intensity upon acidification, in contrast to the LysoTracker probes, which exhibit fluorescence that is largely independent of pH (13). Thus, comparing the distributions of LysoTracker and LysoSensor dyes will indicate the extent of acidification of endosomes. However, when we used both LysoTracker and LysoSensor to stain KO and control MEFs, most of the LysoTracker-positive lysosomes were also positive

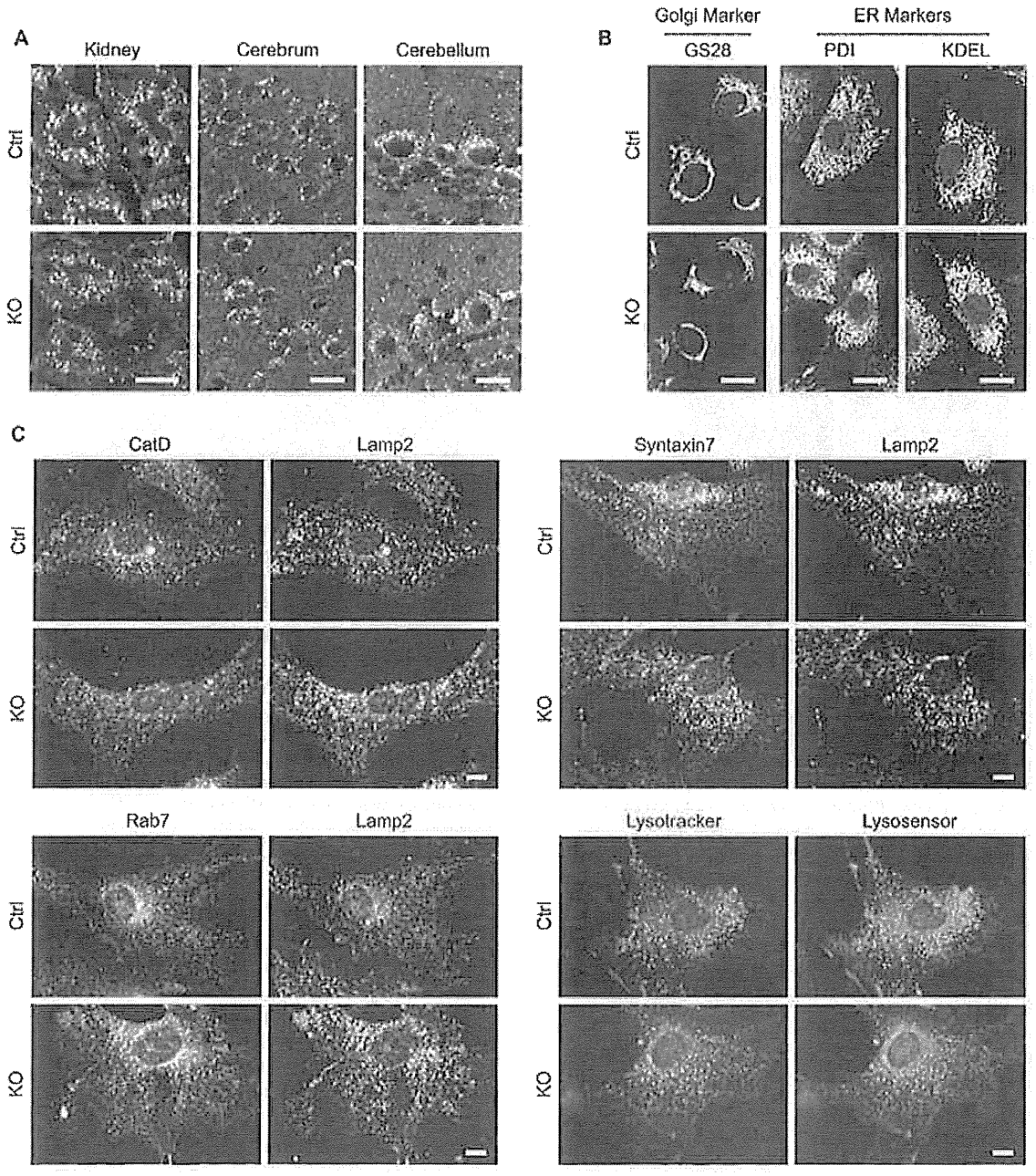

Figure 6: VAMP7 is not essential for the localization of lysosomes and other organelles. A) Immunofluorescence micrographs of kidney, cerebrum and cerebellum from control (Ctrl) and KO mice stained with anti-lamp2 antibody. B) Immunofluorescence micrographs of MEFs from control (Ctrl) and KO mice stained with a Golgi marker (GS28) and two ER markers (PDI and KDEL). C) Immunofluorescence micrographs of MEFs from control (Ctrl) and KO mice double-stained with lamp2 and other lysosomal/late endosomal markers (cathepsin D, Rab7, syntaxin7). Live MEFs were double-stained with LysoTracker and LysoSensor. Merged larger pictures were also presented as Figure S1. Bars, 20 μm.

for LysoSensor and we did not find clear differences in their staining patterns (Figures 6C and S1). We did not find significant changes in the localization or intensity of other organelles such as the Golgi and the endoplasmic reticulum (ER) in KO and control MEFs (Figure 6B).

VAMP7 is not essential for lysosomal exocytosis

VAMP7 is known to mediate Ca^{2+}-regulated lysosomal exocytosis through its interaction with synaptotagmin VII (12). Previous studies showed that deletion of synaptotagmin VII results in impaired lysosomal